

UNCLASSIFIED

AD 409 454

DEFENSE DOCUMENTATION CENTER

FOR

SCIENTIFIC AND TECHNICAL INFORMATION

CAMERON STATION, ALEXANDRIA, VIRGINIA



UNCLASSIFIED

NOTICE: When government or other drawings, specifications or other data are used for any purpose other than in connection with a definitely related government procurement operation, the U. S. Government thereby incurs no responsibility, nor any obligation whatsoever; and the fact that the Government may have formulated, furnished, or in any way supplied the said drawings, specifications, or other data is not to be regarded by implication or otherwise as in any manner licensing the holder or any other person or corporation, or conveying any rights or permission to manufacture, use or sell any patented invention that may in any way be related thereto.

6342

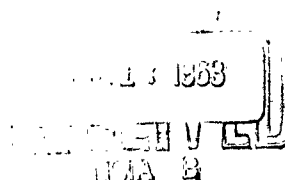
CATALOGED BY DDC
AS AD No. 409454

G|||||||D

FINAL REPORT (1962)

SHELL MODE COUPLING
NOnr 3594(00)
for the
DAVID TAYLOR MODEL BASIN (U)

409454



GENERAL DYNAMICS | ELECTRIC BOAT

FINAL REPORT (1962)

**SHELL MODE COUPLING
NOnr 3594(00)
for the
DAVID TAYLOR MODEL BASIN (U)**

By

**R. J. McGrattan
E. L. North**

The research reported herein was carried out under the Bureau of Ships fundamental hydro-mechanics research program, S-R009 01 01, administered by the David Taylor Model Basin.

Reproduction of this report, in whole or in part, is permitted for any purpose of the United States Government.

Approved by: H. E. Sheets
H. E. Sheets
Director of Research and Development

**U411-63-005
March 1963**

TABLE OF CONTENTS

SECTION	TITLE	PAGE
ABSTRACT		1
LIST OF ILLUSTRATIONS		2
LIST OF TABLES		3
NOMENCLATURE		4
I	INTRODUCTION	5
II	THEORETICAL DEVELOPMENT	7
III	DESCRIPTION OF MATHEMATICAL MODELS	13
	3.1 Comparisons	13
IV	RESULTS	14
V	DISCUSSION AND CONCLUSION	16
VI	REFERENCES	18

ABSTRACT

This report describes a parametric study of stiffened cones and cylinders to analytically determine the effects of a longitudinal steady state driving force on the radial velocity of axially symmetric shells. The "lumped-mass" technique is utilized to predict the natural frequencies, mode shapes and impedances (point and transfer) for eight cases. Although the natural frequencies are not too sensitive to changes in shell thickness and frame area, the transfer impedances (hence radial velocities) vary significantly for the cases studied.

LIST OF ILLUSTRATIONS

FIGURE	TITLE	PAGE
1	Mathematical Model of Stiffened Shell	25
2	Cross Section and Plan View of Unstiffened Shell	26
3	Cross Section and Plan View of Stiffened Shell	27
4	Idealized Mathematical Model for Stiffness Equations	28
5	Shell Geometries	29
6	Frequency Versus Radial Nodes- Case I (1/4" Plate, 2" x 1/2" Stiffener)	30
7	Frequency Versus Radial Nodes- Case II (1/2" Plate, 2" x 1/2" Stiffener)	31
8	Frequency Versus Radial Nodes- Case III (1/4" Plate, 2" x 1" Stiffener)	32
9	Frequency Versus Radial Nodes- Case IV (1/2" Plate, 2" x 1" Stiffener)	33
10	Impedance Plots- Case I (1/4" Plate, 2" x 1/2" Stiffener)-Cylinder	34
11	Impedance Plots- Case II (1/2" Plate, 2" x 1/2" Stiffener)-Cylinder	35
12	Impedance Plots- Case III (1/4" Plate, 2" x 1" Stiffener)-Cylinder	36
13	Impedance Plots- Case IV (1/2" Plate, 2" x 1" Stiffener)-Cylinder	37
14	Impedance Plots- Case I (1/4" Plate, 2" x 1/2" Stiffener)-Cone	38
15	Impedance Plots- Case II (1/2" Plate, 2" x 1/2" Stiffener)-Cone	39
16	Impedance Plots- Case III (1/4" Plate, 2" x 1" Stiffener)-Cone	40
17	Impedance Plots- Case IV (1/2" Plate, 2" x 1" Stiffener)-Cone	41

LIST OF TABLES

TABLE	TITLE	PAGE
1	Comparisons of Parameters	13
2	List of Frequencies and Mode Shapes (Cone)	19
3	List of Frequencies and Mode Shapes (Cylinder)	20
4	Stiffnesses and Impedances for Cone	21
5	Stiffnesses and Impedances for Cylinder	22
6	Effect of Parameter Changes on Impedance Ratios	23
7	Frequency Change for each Parameter Change	24

NOMENCLATURE

m_j	lumped mass at joint j
D_j	deflection at joint j
S_p	stiffness of each member (p)
A	area of member (p)
E	Young's Modulus
μ	Poisson's ratio
l	length of member (p)
I_x, I_y	moments of inertia of member (p)
J	polar moment of inertia of member (p)
K_x, K_y	shear distribution factors
τ	joint (j) restraint factor
x, y	coordinates normal to longitudinal axis
z	longitudinal coordinate
x^1, y^1, z^1	skewed coordinate systems for member (p)
t	time in seconds
ω	eigenvalues
ϕ	eigenvectors
f	natural frequency ($f = \frac{\omega}{2\pi}$ cycles per second).
M	generalized mass
g	gravitational constant (386.4 in/sec ²)

INTRODUCTION

The coupling of shell modes is defined as the interaction of the shell's stretching modes and the shell's lobar modes in a vibrating shell. This interaction affects the sound radiation from the shells when they are subjected to steady state driving forces. Thus, a cylinder being driven along its axis not only creates sound pressure in the direction of the force but also in the radial direction. In this report, the mechanical coupling of the modes is investigated but not the resulting sound radiation.

Lobar frequencies of shells are usually calculated separately from the stretching frequencies for the sake of simplifying the calculations. But to determine the true interaction between the two, they must be considered simultaneously. To facilitate the latter, a computer program was developed [1, 2, 3, & 4]* that can calculate the frequencies, mode shapes, and mechanical impedances of a shell of any (arbitrary) geometry. The technique used is commonly called the "lumped-mass" method. By this is meant that structural systems, in this case stiffened cylinders and cones, are idealized as a grid-work of plates and beams whose masses are concentrated at their respective centers of gravities. In the case of a stiffened cylinder, the gridwork consists of a series of flat plates (Fig. 1) related by direction cosines to form the shell, and straight beam members, also related by direction cosines, to form the stiffeners. Continuity and equilibrium are satisfied at the joints between members. Thus the stiffness (and flexibility) of the entire structure can be determined, and having established the mass distribution, the equations of motions can be written and solved to determine natural frequencies and mode shapes. The point and transfer impedances can then be determined.

* Refers to references (pg 18)

In this study, the objective is to determine the natural frequencies, mode shapes, and impedances of two basic shells of revolution: cylinders and cones. After choosing the diameters and lengths, several combinations of shell thicknesses and stiffener areas were considered. The results indicate to what extent frame size and shell thickness influence the vibrational behavior of cylinders and cones, which in turn influences the nature and strength of the sound radiation from these shells. Ultimately, a thorough knowledge of the effects of the shell and stiffener geometry on the vibration and radiation characteristics can lead to structures with minimal adverse behavior.

II

THEORETICAL DEVELOPMENT

The initial operation in analyzing stiffened shells (Fig. 1a) by the lumped mass technique is to idealize the shell and stiffeners by a system of flat plates and bars (Fig. 1b). Hrennikoff[5] has shown that the flexibility of this system can be duplicated by using a mathematically equivalent framework of elastic bars (Fig. 1c). This equivalent framework is then used as the mathematical model for the structure.

Each member of the framework has typical beam properties, but these properties are mathematical equivalents only, and do not have direct physical meaning. A typical cross section and plan view of an unstiffened shell are shown in Figs. 2a and 2b.

The properties of the members in these panels are:

$$\begin{aligned}
 A_0 &= \frac{3}{8} \left[\frac{3K^2 - 1}{K} \right] \text{ at } & I_{x0} &= \left[A_0 \frac{t^2}{12} \right] \cos^2 \alpha \\
 A_1 &= \frac{3}{8} \left[3 - K^2 \right] \text{ at } & I_{yo} &= \left[A_0 \frac{t^2}{12} \right] \sin^2 \alpha \\
 A_2 &= \frac{3}{16} \left[\left(\frac{1 + K^2}{K} \right)^{\frac{3}{2}} \right] \text{ at } & I_{x1} &= A_1 \frac{t^2}{12} \\
 && I_{x2} &= A_2 \frac{t^2}{12}
 \end{aligned}$$

The addition of a stiffener (Figs. 3a and 3b) contributes to the stiffness of the circumferential frames.

The only properties which change are A_1 and I_{x1} :

$$A_{1s} = A_0 + A_{(\text{frame})}$$

$$I_{x1s} = I_{x1} + I_x(\text{frame})$$

$$I_{y1} = I_y(\text{frame})$$

Since the amount of damping inherent to thin shells is very small compared with the value for critical damping, the effects on the natural frequencies and mode shapes are negligible. Thus, the only parameters needed to determine the natural frequencies are the structural geometry, mass distribution and end conditions, which are all determined in establishing the equivalent gridwork of elastic beams.

The equations of motion for free vibrations are:

$$m_j \ddot{D}_j + \sum_{i=1}^n S_{ji} D_i = 0 \quad (1)$$

where j is the joint number.

Each joint (j) is common to two or more members (p), and the joint stiffness (S_{jj}) is comprised of the sum of the stiffnesses of each member (S_p). The stiffness of each member at the centroid of the member is:

$$S_p = \begin{bmatrix} a_{11} & & & & & 0 \\ a_{21} & a_{22} & & & & \\ & a_{32} & a_{33} & & & \\ & & a_{43} & a_{44} & & \\ & & & a_{54} & a_{55} & \\ 0 & & & & a_{65} & a_{66} \end{bmatrix} \quad (1.1)$$

where

$$a_{11} = \frac{AE}{\ell}$$

$$a_{22} = 12 EI_x A / [\ell^3 A + 24(1 + \mu)K_x \ell I_x]$$

$$a_{33} = 12 EI_y A / [\ell^3 A + 24(1 + \mu)K_y \ell I_y]$$

$$a_{44} = JQ/(1 - \tau)l$$

$$a_{55} = EI_y/l$$

$$a_{66} = EI_x/l$$

Before the stiffnesses of each member (S_p^o) are summed to get the joint stiffness (S_{jj}), each member's stiffness is rotated and translated from its own coordinate system to the coordinate system of a common origin.

Thus:

$$S_p^o = L^T B S_p B^T L \quad (1.2)$$

where

$$L = \begin{bmatrix} K_{1z} & 0 \\ 0 & K_{1z} \end{bmatrix} \quad (1.3)$$

$$K_{1z} = \begin{bmatrix} \cos x^1 x & \cos x^1 y & \cos x^1 z \\ \cos y^1 x & \cos y^1 y & \cos y^1 z \\ \cos z^1 x & \cos z^1 y & \cos z^1 z \end{bmatrix}$$

$$B = \begin{bmatrix} 1 & & & & & 0 \\ 0 & 1 & & & & \\ 0 & 0 & 1 & & & \\ 0 & (z_p - z_o) & (y_o - y_p) & 1 & & \\ (z_o - z_p) & 0 & (x_p - x_o) & 0 & 1 & \\ (y_p - y_o) & (x_o - x_p) & 0 & 0 & 0 & 1 \end{bmatrix} \quad (1.4)$$

Once the stiffnesses of all the joints are calculated at the origin, they can be used to form the stiffness matrix and the $\sum_{i=1}^n S_{ji} D_i$ matrix in the equation of motion.

$$\sum_{i=1}^n S_{ji}^o D_i = S_{jj}^o D_j - \sum_{k=1}^n S_{jk}^o D_k^o \quad (2)$$

$K \neq j$

Thus, in (Fig. 4)

$$\sum_{i=1}^n S^o_{ji} D^o_i = \begin{bmatrix} [S_1^o + S_2^o + S_3^o] & -S_1^o & 0 & -S_2^o & \dots \\ -S_1^o & [S_1^o + S_4^o + S_5^o] & -S_5^o & -S_4^o & \dots \\ \vdots & \vdots & \vdots & \vdots & \vdots \\ \text{etc.} & \text{etc.} & \text{etc.} & \text{etc.} & \text{etc.} \end{bmatrix} \begin{bmatrix} D_A^o \\ D_B^o \end{bmatrix} \quad (2.1)$$

Or, in matrix form

$$\sum_{i=1}^n S^o_{ji} D^o_i = S^o D^o \quad (2.2)$$

where S^o is the $n \times n$ stiffness matrix at the origin
and D^o is the $n \times 1$ deflection vector at the origin

Before the natural frequencies of the system are calculated, the stiffness matrix at the origin (S^o) is inverted to form an influence coefficient matrix (δ^o).

$$[S^o]^{-1} = \delta^o \quad (2.3)$$

The influence matrix forms the characteristic matrix and is transferred back to the initial coordinate system at the joints.

$$\delta = B^T L^T F^T \delta^o L B F \quad (2.4)$$

F is a force matrix with unit forces at each mass for each degree of freedom.

The equations of motion then can be written in terms of the influence coefficient matrix:

$$\ddot{D} = -\delta M \dot{D} \quad (3)$$

where:

D is the displacement vector ($6n \times 1$)

\ddot{D} is the acceleration vector ($6n \times 1$)

δ is the flexibility matrix ($6n \times 6n$)

M is the diagonal mass matrix ($6n \times 6n$)

The natural frequencies can be determined by assuming a periodic displacement

$$D = \phi \sin \omega t \quad (3.1)$$

and inserting into equation (3) to get the frequency equation:

$$\left[\frac{I}{\omega^2} - \delta M \right] = 0 \quad (4)$$

A more expedient form of equation (4) is obtained if the mass matrix is factored so that:

$$M = \lambda^T \lambda \quad (4.1)$$

where:

$$\lambda = \begin{bmatrix} \sqrt{m_1} & & & & & 0 \\ & \ddots & & & & \\ & & \sqrt{m_1} & & & \\ & & & \ddots & & \\ 0 & & & & \ddots & \\ & & & & & \sqrt{m_n} \end{bmatrix} \quad (4.2)$$

Premultiplying equation (4) by λ and using (4.1) results in:

$$\left| \frac{I}{\omega^2} - \lambda \delta \lambda^T \right| = 0 \quad (5)$$

Since $\lambda \delta \lambda^T$ is a symmetrical matrix, computer storage for only half of the non-diagonal terms is required.

The solution of equation (5) is accomplished by using the Modified Givens Method [6] to determine the eigenvalues (ω) and eigenvectors (θ). Due to the operation whereby $\lambda \delta \lambda^T$ is used, the eigenvectors are not the true ones, but are reorientated. The true eigenvectors are then obtained by:

$$\varphi = \lambda^{-1} \theta \quad (6)$$

The equation for the undamped transfer and point impedances, using the eigenvalues (ω) and eigenvectors (φ) of the stiffened shell, is

$$Z_{jk} = \frac{1}{\frac{\sum_{r=1}^n \varphi_j \varphi_k \omega_r^2}{M}} \quad (7)$$

, where $j = k$ for point impedance.

III

DESCRIPTION OF MATHEMATICAL MODELS

Eight models were analyzed, four cones and four cylinders (Fig. 5). For all cases, the end conditions were the same; zero radial deflection, zero longitudinal slope and free longitudinally at the end with the steady state driving force ($F_{e \text{ int}}$). The length and diameter of the cylinder were held constant, and the shell thickness and area of frames were varied. Similarly, in the cone the length and diameter were held constant and the shell thickness and areas of frames were varied.

Since four cases were studied for each the cone and cylinder, six comparisons can be made for each geometry (Table 1). In both the cone and cylinder, two shell thicknesses and two areas of frame were considered. Therefore, the cases to be compared are:

3.1 Comparisons

TABLE I

- a. Doubling the frame area (1 in^2 to 2 in^2) while keeping shell thickness constant ($1/4 \text{ in}$).
- b. Doubling the frame area (1 in^2 to 2 in^2) while keeping shell thickness constant ($1/2 \text{ in}$).
- c. Doubling the shell thickness ($1/4 \text{ in}$ to $1/2 \text{ in}$) while keeping the frame area constant (1 in^2).
- d. Doubling the shell thickness ($1/4 \text{ in}$ to $1/2 \text{ in}$) while keeping the frame area constant (2 in^2).
- e. Doubling both the shell thickness ($1/4 \text{ in}$ to $1/2 \text{ in}$) and frame area (1 in^2 to 2 in^2).
- f. Doubling the shell thickness ($1/4 \text{ in}$ to $1/2 \text{ in}$) while halving the frame area (2 in^2 to 1 in^2).

IV

RESULTS

The most significant variations in results for the cases of cones and cylinders were in the impedances (point and transfer). The transfer impedances are the most important to this study, since they determine the longitudinal steady state driving force required to impart a unit velocity to either the shell plating or frames in a radial direction.

For each of the four cases of cylinders and cones, the point and transfer impedances were determined at the center stiffener and at a point on the shell midway between the center stiffener and the adjacent stiffener (Figs. 10 through 17). Since the lower lobar modes ($m = 1, n = 2, 3, 4$) are the most efficient sound radiators, the impedances for these modes are most significant. Tables 4 and 5 give the stiffnesses ($K = i\omega Z$) and impedances (point and transfer) for the lower modes for the various cases of cylinders and cones.

Table 6 compares ratios of transfer impedances and shows that the cones and cylinders react differently to the parameter changes. The highest increase in the cylinders is derived by increasing the shell thickness (comparison c & d) whereas the highest increase in the cone is derived by increasing the frame area (comparison a & b).

Contrary to the impedance results, the percent changes in frequencies (stretching and lobar) are not too sensitive to the changes in shell thickness and frame areas. For each case, there are approximately 25 frequencies below 1 kc(10^3 cps). The frequencies for the first four longitudinal modes ($m = 1, 2, 3, 4$) and first six lobar modes ($n = 2, 3, 4, 5, 6$) are shown in Tables 2 and 3. The percent changes in frequencies are shown in Table 7.

For both the cylinders and cones, the largest increase in frequencies for the lowest lobular modes ($m = 1, n = 1, 2$) can be derived by increasing the shell thickness and decreasing the area of frames (comparison f of Table 1).

The analyses of the cones also revealed that the lobular mode shapes in some cases are "mixed" (see figures 6, 7, 8, 9). In some cases the frames and shells have different mode shapes while in other cases the shell and frames at one end of the cone have different mode shapes from that of the shell and frames at the other end.

The percent changes in frequency for the lobular modes (n) decrease with longitudinal modes (m) for both the cones and cylinders. The fourth longitudinal mode ($m = 4$) has the smallest change. Since the half-wave-length for this mode approximately equals the length between frames, the shell behaves somewhat as an unstiffened shell and thus the changes in frequency would expectedly be small.

V

DISCUSSION AND CONCLUSION

For the cases studied, the variations in shell thickness and frame area have their greatest effects on the transfer impedances. Thus, it is apparent that the radial velocity of both shell and frames can be significantly reduced by an expedient choice of frame area and shell thickness. The effect of frame spacing was not investigated in this study, but it would also have a significant effect.

Considering the two parameters studied (shell thickness and frame area) the most efficient way of raising the transfer impedances (thus reducing the radial velocity) in the cylinder is to keep the area of frames constant while increasing the shell thickness. In the cones, however, the opposite is true. The most effective means of increasing the transfer impedances are to keep the shell thickness constant while increasing the frame area.

Unlike the large variation in impedances, the natural frequencies (stretching and lobar) do not substantially change for all the cases of cylinders and cones. The greatest changes are accomplished by increasing the shell thickness while decreasing the frame area.

One of the most significant results is the fact that in the cones there exist "mixed" lobar modes. These "mixed" modes start as low as the fourth mode and take two forms; in some cases the mode shapes at either end of the cone differ, and in others the shell has one mode shape while the frames have another. The significance of these phenomena is that only an analytic method that does not predetermine a mode shape (such as the lumped mass methods) will determine these modes. Since the "lumped mass" technique used is valid for any geometry, symmetrical as well as not, this method can determine these "mixed" modes with equal facility as well as the regular lobar modes.

The results of this study indicate that expedient shell designs can significantly reduce the radial velocity of the shells when subjected to steady state longitudinal driving force.

REFERENCES

- 1) L. H. Chen, J. Cadoret and C. Aldrich, "A Matrix Method for Analysis of Complex Structures", Electric Boat Division Report P59 - 035, dated February 1959.
- 2) R. Christensen and J. Cadoret, "Plate Vibration Studies", Electric Boat Division Report, TSD59 - 251, dated December 1959.
- 3) J. Catlin and R. McGrattan, "Sound Radiation from a Cylindrical Shell", U413-61-210, Final Report (1961) for David Taylor Model Basin Contract NOnr 3280(00), dated December 1961.
- 4) V. H. Neubert and W. H. Ezell, "Dynamic Behavior of Foundation-Like Structures", - Colloquium on Mechanical Impedance Methods - ASME - dated December 1958.
- 5) A. Hrennikoff, "Solutions of Problems of Elasticity by the Frame-Worthy Method", Journal of Applied Mechanics, page A-169, December 194.
- 6) E. Bodewig, "Matrix Calculus", Interscience Publishers, Inc., New York, 1956, p. 280 and 287.

TABLE 2
LIST OF FREQUENCIES AND MODE SHAPES (CONE)

Case 1			Case 2			Case 3			Case 4		
$1/4 \pi$ 2x1/2S			$1/2 \pi$ 2x1/2S			$1/4 \pi$ 2x1S			$1/2 \pi$ 2x1S		
(FREQ. cps)	m	n	(FREQ. cps)	m	n	(FREQ. cps)	m	n	(FREQ. cps)	m	n
322	1	2	312	1	2	290	1	2	307	1	2
337	1	3	324	1	3	373	1	3	349	1	3
358	1	4	356	1	4	447	1	4	410	1	4
429	1	5/3	424	1	3/5	514	1	3/5	480	1	3/5
440	1	6/4	442	1	6	530	1	4/6	503	1	6
511	2	3/5	476	2	4	549	2	4	527	2	4
464	2	4	523	2	3/5	549	2	3/5	555	2	3
561	2	3/5	547	2	6	566	2	2	596	2	5/3
528	2	6	576	2	3	598	2	6	606	2	6
588	3	6	635	3	4	607	2	5	613	2	2
605	3	5	644	2	2	622	3	6	661	3	4
599	3	4	647	3	5	639	3	5	679	8	
649	2	6/4	654	3	6	640	8		687	3	5
681	8		703	8		650	3	4	697	3	6
669	4	6/2	731	4	6	676	4	4/6	732	4	6
706	4	5	750	4	3/5	705	3	3/5	754	4	5
761	3	3	801	3	3	728	4	3/5	773	3	5/3
763	4	4	806	4	4	770	4	4	808	4	4
870	5	6	920	3	2	784	3	2	871	3	2
889	5	5	928	5	6	889	5	4	939	5	5
933	4	3	930	5	5	916	5	3/5	942	5	4
971	3	2	976	4	3	988	4	3	968	4	3

TABLE 3
LIST OF FREQUENCIES AND MODE SHAPES (CYLINDER)

Case 1			Case 2			Case 3			Case 4		
1/4 E FREQ (cps)	2x1/2S m n		1/2 E FREQ (cps)	2x1/2S m n		1/4 E FREQ (cps)	2x1S m n		1/2 E FREQ (cps)	2 x 1S m n	
252	1 3		263	1 3		266	1 3		270	1 3	
306	1 2		319	1 2		285	1 2		308	1 2	
361	1 4		340	1 4		413	1 4		397	1 4	
456	1 5		437	1 5		493	2 3		503	1 5	
475	2 4		473	1 6		502	2 4		506	2 4	
486	1 6		474	2 4		515	1 5		538	1 6	
518	2 5		517	2 5		543	1 6		543	2 3	
544	2 6		543	2 6		567	2 5		582	2 5	
554	2 3		575	2 3		576	2 2		592	2 6	
616	S		636	S		583	S		617	S	
629	2 2		655	3 4		586	2 6		630	2 2	
635	3 4		661	2 2		613	3 5		665	3 4	
646	3 6		662	3 5		633	3 4		686	3 5	
649	3 5		663	3 6		666	3 6		689	3 6	
711	4 6		744	4 6		668	3 3		731	3 3	
720	3 3		764	3 3		709	4 5		747	4 6	
736	4 5		766	4 5		715	4 6		768	4 5	
793	4 4		818	4 4		767	3 2		821	4 4	
837	3 2		880	3 2		793	4 4		839	3 2	
890	5 4		921	4 3		835	5 5		923	4 3	
905	4 3		940	5 4		863	5 4		923	5 4	
920	5 3					896	4 3				
926	5 5										

CONE

CASE	PLATE	STIFFENER	STIFFNESS ($\frac{lb}{in}$)			IMPEDANCE ($\frac{lb\cdot sec}{in}$)		
			LONG. TO PL.	LONG. TO STIFF. ST.	Z (POINT) PL.	Z (POINT) ST.	Z _{Trans, E}	Z _{Trans, ST.}
(1) $\frac{1}{4} E, 2x1/2S$	$9x10^4$	$2.5x10^5$	$6.4x10^6$	$1.1x10^7$	(2) (3) (4) 3.2 1.8 3.3	3.3 3.0 1.8	14 9.9 28	17 16 48
(2) $\frac{1}{2} E, 2x1/2S$	$1.9x10^5$	$4.1x10^5$	$1x10^7$	$1.3x10^7$	(2) (3) (4) 2.4 5.5 5.5	1.7 2.5 2.7	36 11 90	6. 15 39
(3) $\frac{1}{4} E, 2x1S$	$1.3x10^5$	$4x10^5$	$5.1x10^6$	$1.4x10^7$	(2) (3) (4) 4.8 2.3 2.1	5.0 3.8 28	32 23 900	80 36 1700
(4) $\frac{1}{2} E, 2x1S$	$2.2x10^5$	$5.6x10^5$	$1.1x10^7$	$1.5x10^7$	(2) (3) (4) 3.8 4.0 9.0	7.3 2.3 20.0	100 140 420	26 27 220

TABLE 4 STIFFNESSES AND IMPEDANCES FOR CONE

TABLE 5 STIFFNESSES AND IMPEDANCES FOR CYLINDER

CYLINDER

STIFFNESS (1b/in)				IMPEDANCE ($\frac{1b\text{-sec}}{in}$)				
CASE	PLATE	STIFFENER	LONG. TO PL.	LONG. TO STIFF.	Z _{PL.}	Z _{ST.}	Z _{TRAN, H.}	Z _{TRAN, ST.}
1 1/4 E, 2x1/2S	9.9x10 ⁶	3.2x10 ⁶	1.2x10 ⁷	8.2x10 ⁶	(3) (2) (4)	5.6 3.7 2.1	8 12 20	420 46 270
2 1/2 E, 2x1/2S	2.3x10 ⁵	5.6x10 ⁵	1.7x10 ⁷	1.9x10 ⁷	(3) (2) (4)	8.7 8.6 6.9	18 17 20	650 270 420
3 1/4 E, 2x1S	1.3x10 ⁵	4.4x10 ⁵	9.0x10 ⁶	7.0x10 ⁶	(3) (2) (4)	3.3 8 7	6.2 21 29	100 78 101
4 1/2 E, 2x1S	2.7x10 ⁵	7.6x10 ⁵	3.8x10 ⁷	2.3x10 ⁷	(3) (2) (4)	8.8 3.6 11.0	13 23 41	470 130 240
								360 210 890

COMPARISON	CYLINDER				CONE			
	NODES*	Z _{TP}	Z _{TS}	NODES*	Z _{TP}	Z _{TS}		
a	3	0.24	0.24	2	2.3	4.7		
	2	1.7	4.0	3	2.6	2.2		
	4	0.37	14	4	32	35		
b	3	0.72	0.53	2	2.8	4.3		
	2	0.48	1.2	3	13	1.8		
	4	0.57	24	4	4.7	5.6		
c	3	1.6	2.0	2	2.6	0.37		
	2	4.9	4.1	3	1.1	0.94		
	4	1.6	11	4	3.2	0.81		
d	3	4.7	4.4	2	3.1	0.33		
	2	1.6	1.2	3	6.1	0.75		
	4	2.4	2.8	4	0.47	0.13		
e	3	1.1	1.1	2	7.1	1.5		
	2	2.8	7.4	3	14	1.7		
	4	0.89	40	4	15	4.6		
f	3	6.5	8.3	2	1.1	0.076		
	2	3.5	1.0	3	0.48	0.42		
	4	4.2	0.81	4	0.1	0.023		

* m = 1

TABLE 6
EFFECT OF PARAMETER CHANGES ON IMPEDANCE RATIOS

TABLE 7 FREQUENCY CHANGE FOR EACH PARAMETER CHANGE (cps/%)

m-n	Comp.	1-2	1-3	1-4	1-5	1-6	2-2	2-3	2-4	2-5	2-6	3-2	3-3	3-4	3-5	3-6	4-2	4-3	4-4	4-5	4-6
a	-21	14	52	59	57	-53	-61	27	49	42	-70	-52	-2	-36	20	-9	0	-27	4		
	-7%	6%	14%	13%	12%	-8%	11%	6%	10%	8%	-8%	-7%	0%	-6%	3%	-1%	0%	-3%	1%		
	-11	7	57	66	65	-31	-32	32	65	49	-41	-33	10	24	26	2	3	2	3		
	-3%	3%	17%	15%	14%	-5%	-6%	7%	13%	9%	-5%	-4%	2%	4%	4%	0%	0%	0%	0%		
	13	11	-21	-19	-13	32	21	-1	-1	43	44	20	13	17	16	25	30	30	33		
	4%	4%	-6%	-4%	-3%	5%	4%	0%	0%	0%	5%	6%	3%	2%	3%	2%	3%	4%	5%		
b	23	4	-16	-12	5	54	50	4	15	6	72	63	32	73	23	27	28	59	32		
	8%	2%	-14%	-2%	1%	9%	10%	1%	3%	1%	9%	9%	5%	12%	4%	3%	4%	8%	5%		
	2	18	36	47	52	1	-11	31	64	48	2	11	30	37	43	18	28	32	36		
	e	1%	7%	10%	10%	11%	0%	-2%	7%	12%	9%	0%	2%	5%	6%	7%	2%	4%	4%	5%	
	34	-3	-73	-78	-70	85	82	-28	-50	-43	113	96	22	49	-3	25	25	57	29		
	f	12%	-1%	-18%	-15%	-13%	13%	15%	17%	6%	3%	-7%	15%	14%	4%	8%	1%	3%	3%	4%	
m-n	Comp.	1-2	1-3	1-4	1-5	1-6	2-2	2-3	2-4	2-5	2-6	3-2	3-3	3-4	3-5	3-6	4-2	4-3	4-4	4-5	4-6
a	-36	89	85	90	-83	-12	85	38	70	-187	-56	-51	34	34	55	9	22	7			
	-10%	11%	25%	20%	21%	-13%	-2%	18%	7%	13%	-19%	-7%	-9%	6%	6%	6%	1%	3%	1%		
	-5	25	54	56	61	-31	32	51	73	59	-49	-28	26	40	43	-8	2	4	1		
	-2%	8%	15%	13%	14%	-5%	6%	11%	14%	11%	-5%	-3%	4%	6%	7%	-1%	0%	1%	0%		
	-10	-13	-2	-5	2	-5	15	12	12	19	-51	40	36	42	66	43	43	44	62		
	c	17	-24	-37	-34	-27	47	6	-22	-11	8	87	68	11	48	75	5%	6%	6%	9%	
d	6%	-6%	-8%	-7%	-1%	1%	3%	2%	4%	-5%	5%	5%	6%	7%	11%	-20	38	26	56		
	-15	12	52	51	63	-36	-6	63	85	78	-100	12	62	82	109	35	45	48	63		
	e	-5%	4%	15%	15%	12%	14%	-6%	-1%	14%	17%	15%	-10%	14%	19%	4%	6%	7%	9%		
	22	-49	-91	-90	-88	-78	27	-73	-84	-51	136	96	-15	8	32	-12	36	22	55		
	f	8%	-13%	-20%	-18%	-17%	14%	5%	-13%	-14%	-8%	17%	14%	-2%	1%	5%	-10%	5%	3%	8%	

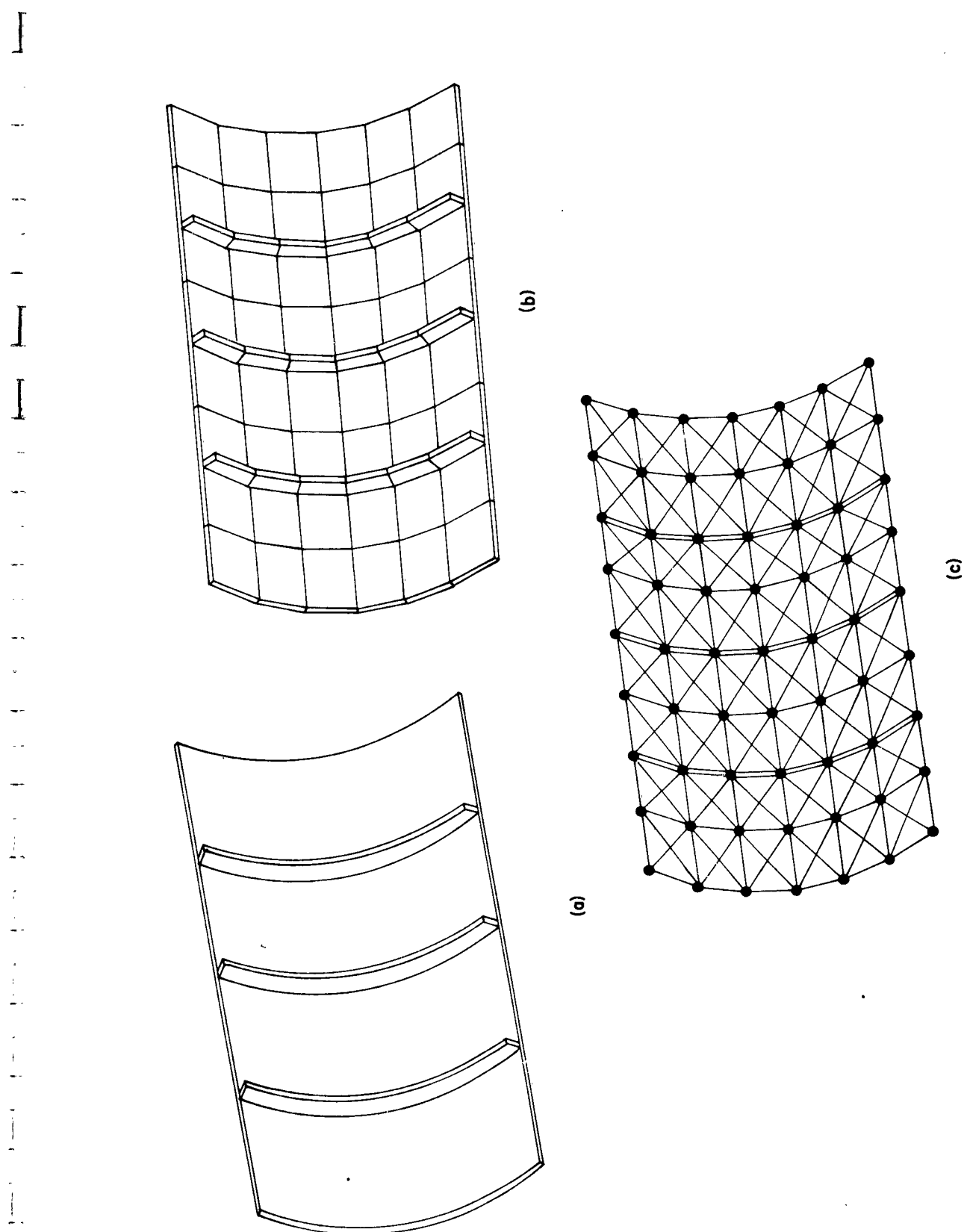
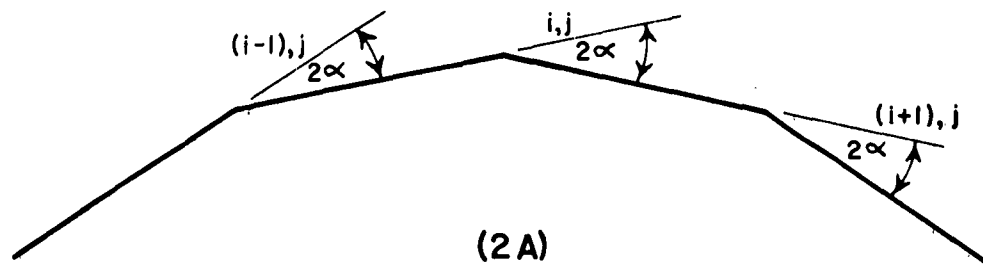
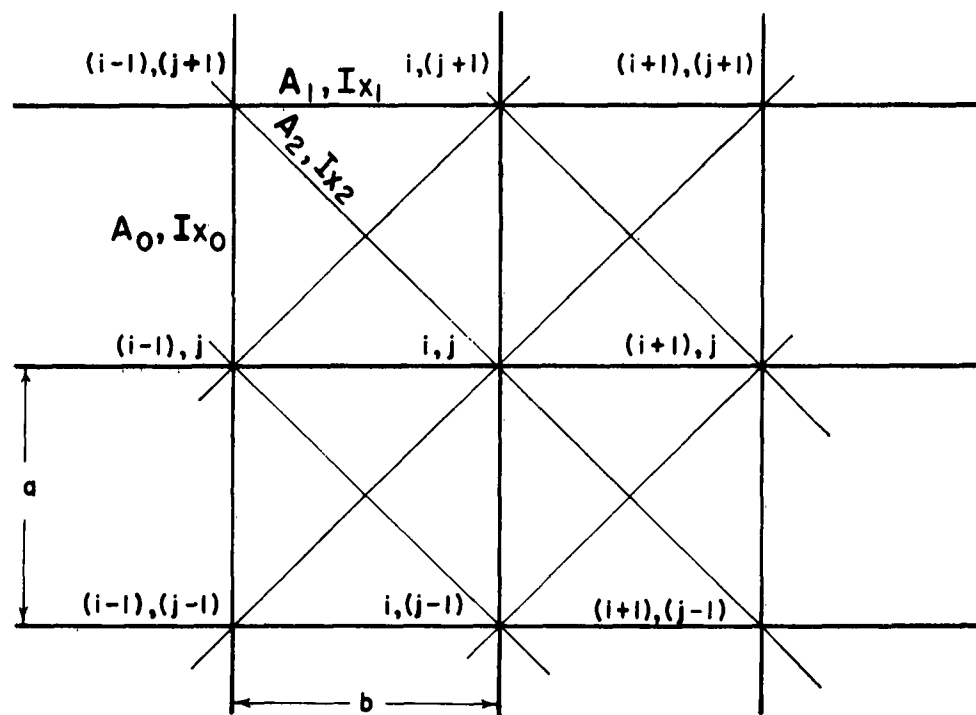


FIGURE 1 MATHEMATICAL MODEL OF STIFFENED SHELL

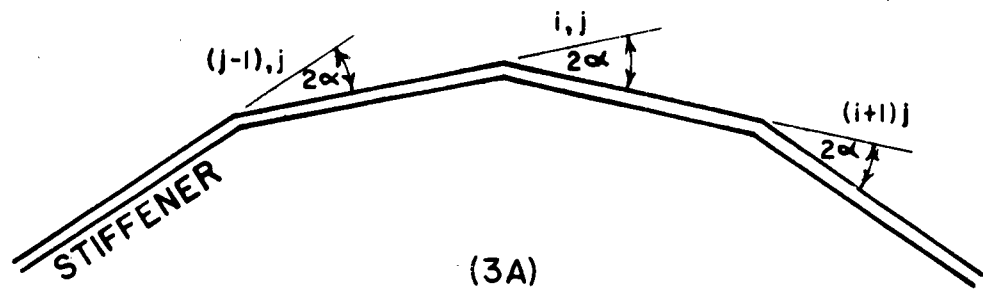


(2A)

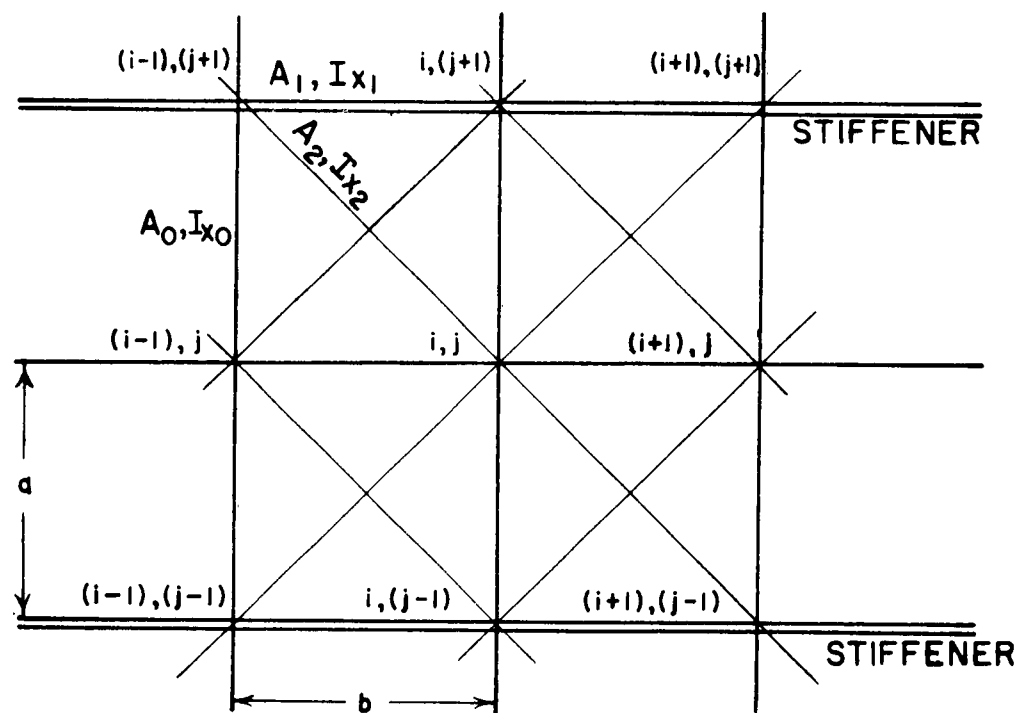


(2B)

FIGURE 2 CROSS SECTION AND PLAN VIEW OF UNSTIFFENED SHELL



(3A)



(3B)

FIGURE 3 CROSS SECTION AND PLAN VIEW OF STIFFENED SHELL

FIGURE 4

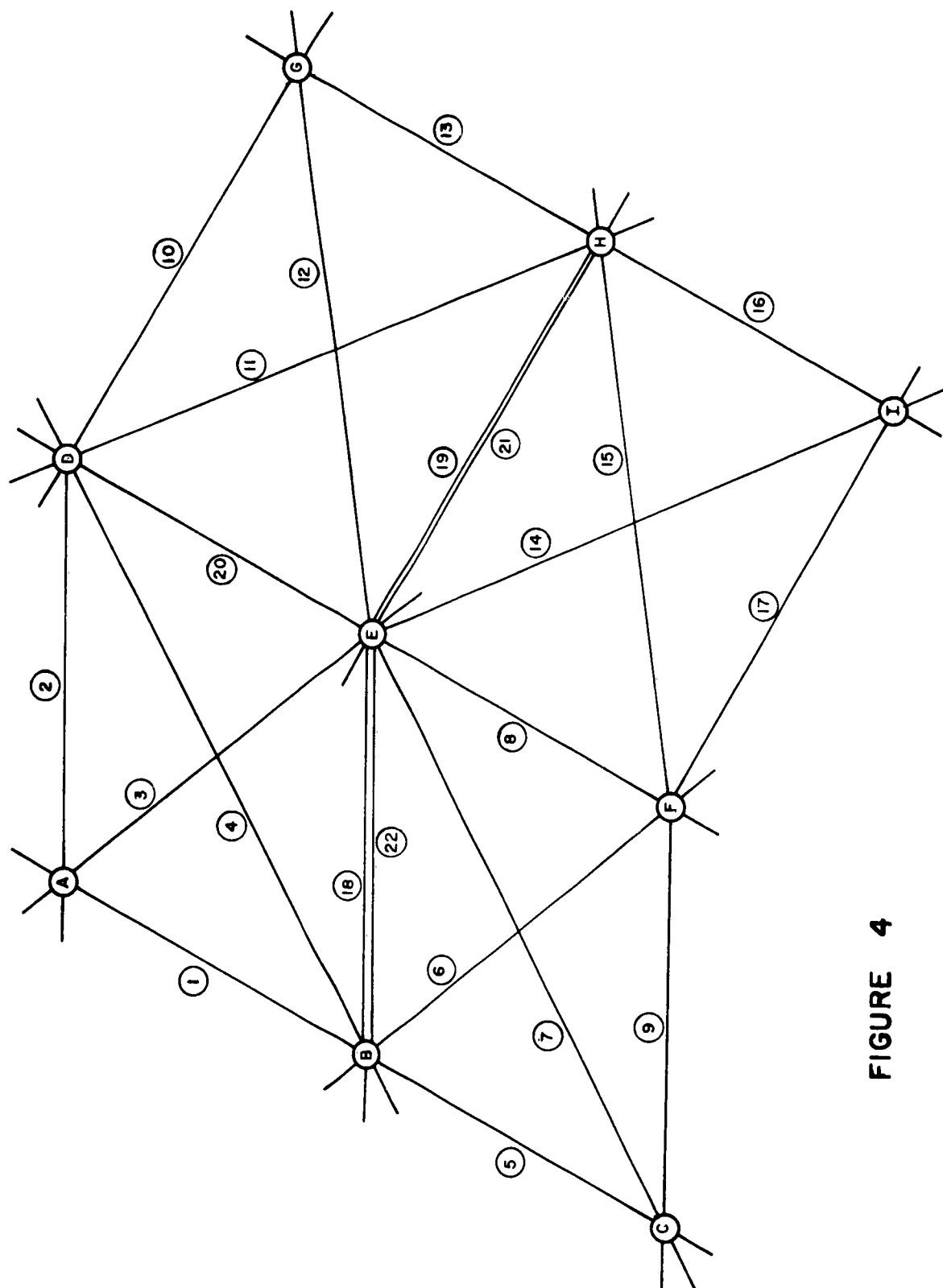


FIGURE 4 IDEALIZED MATHEMATICAL MODEL FOR STIFFNESS EQUATIONS

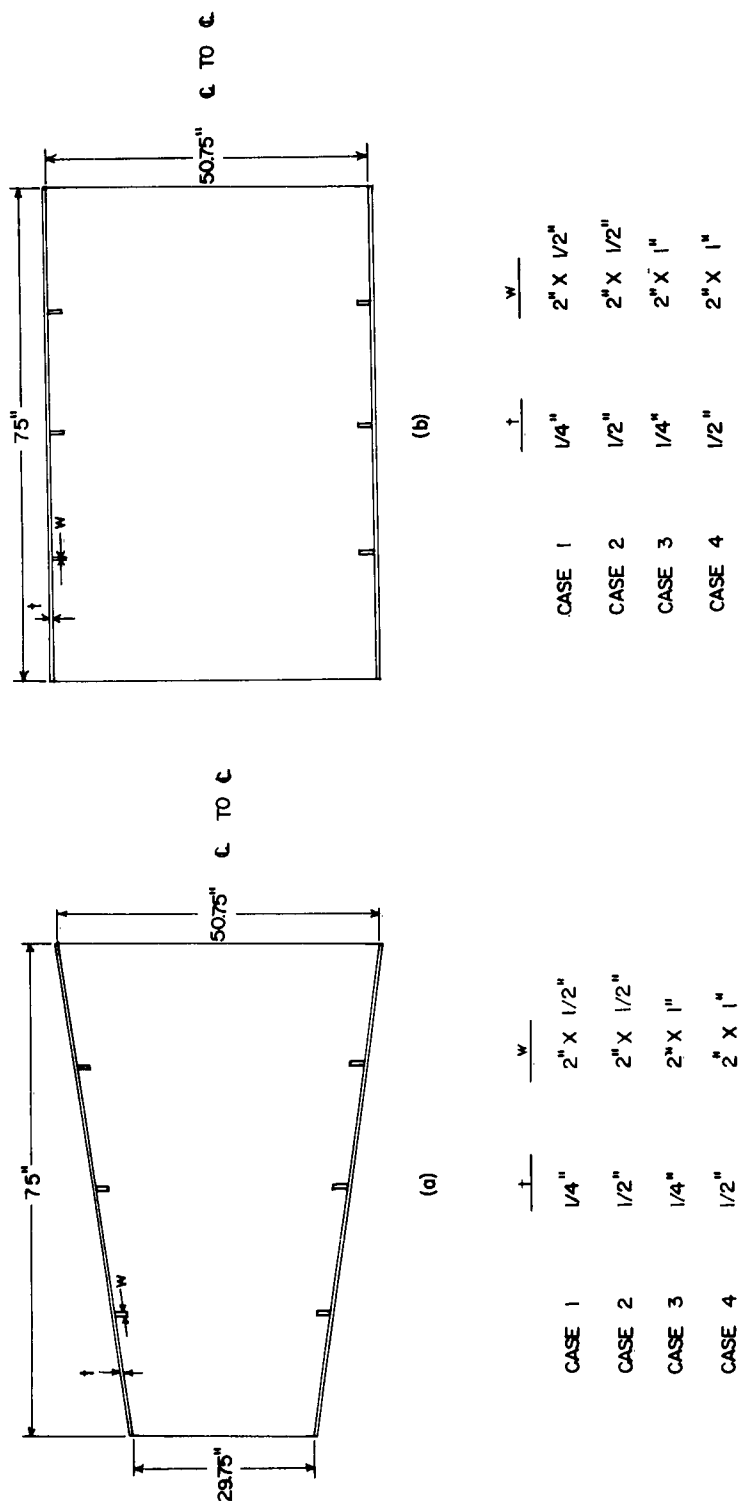


FIGURE 5 SHELL GEOMETRIES

1/4" PLATE
2" X 1/2" STIFFENER

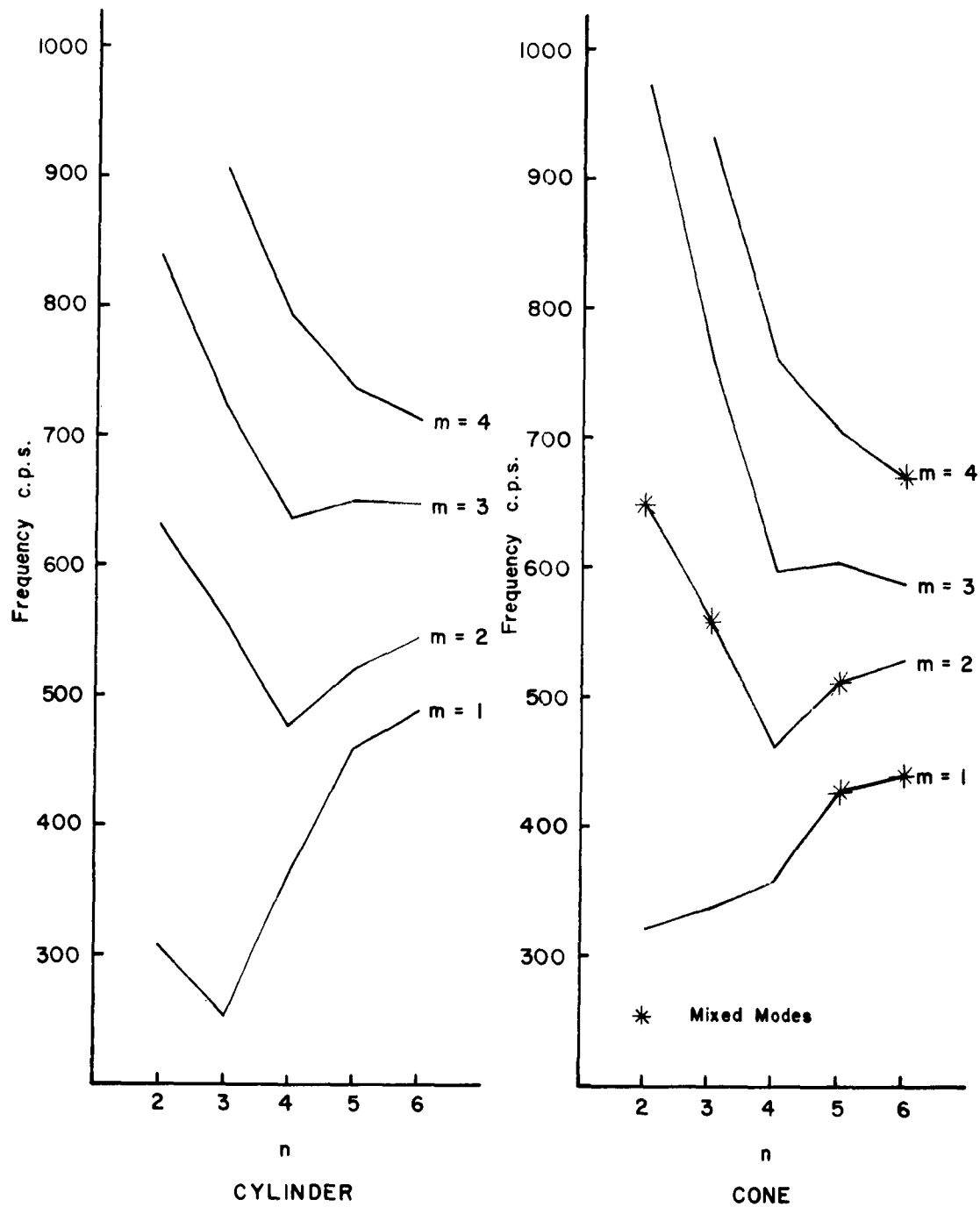


FIGURE 6 FREQUENCY VERSUS RADIAL NODES

1/2" PLATE
2" X 1/2" STIFFENER

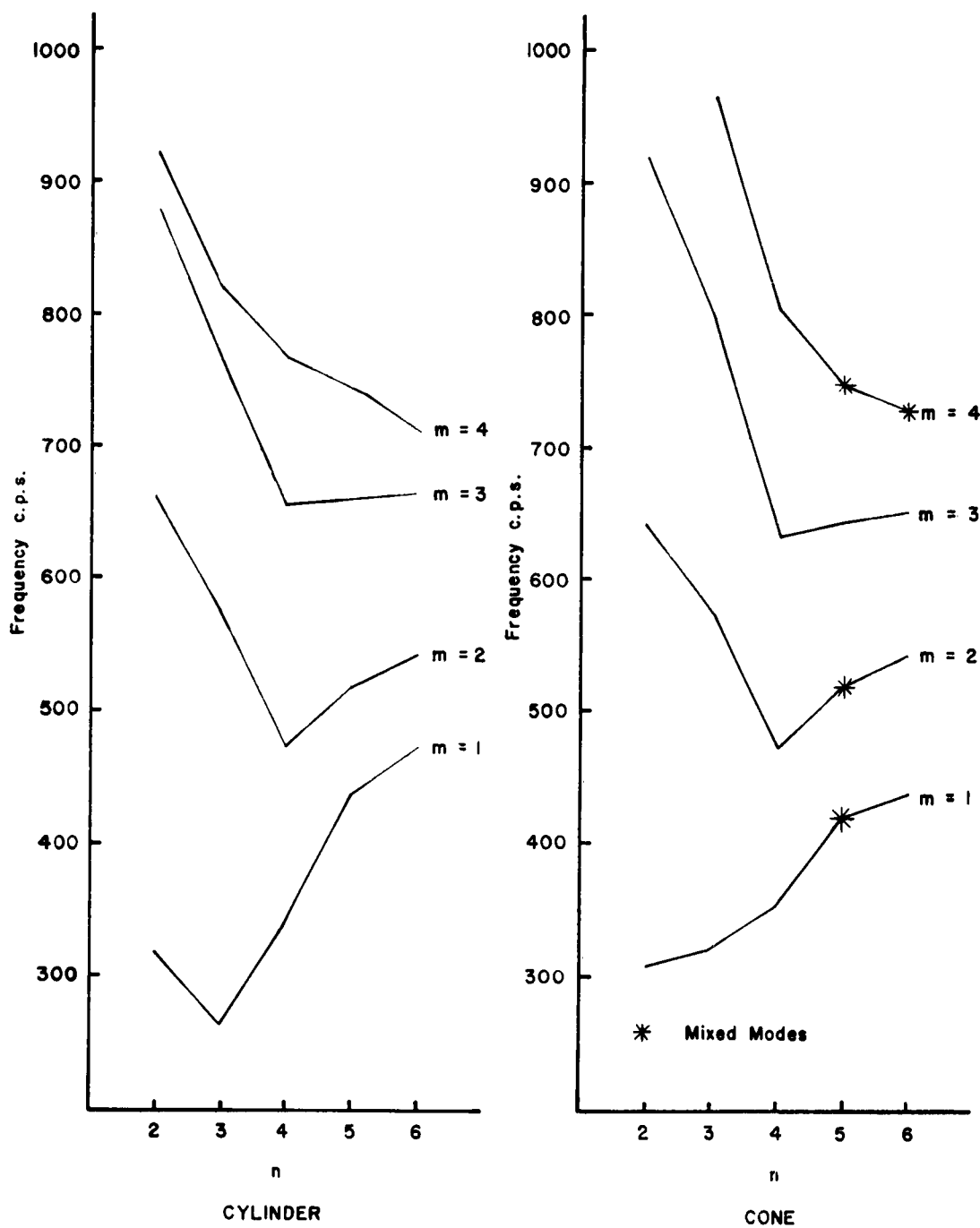


FIGURE 7 FREQUENCY VERSUS RADIAL NODES

1/4" PLATE
2" X 1" STIFFENER

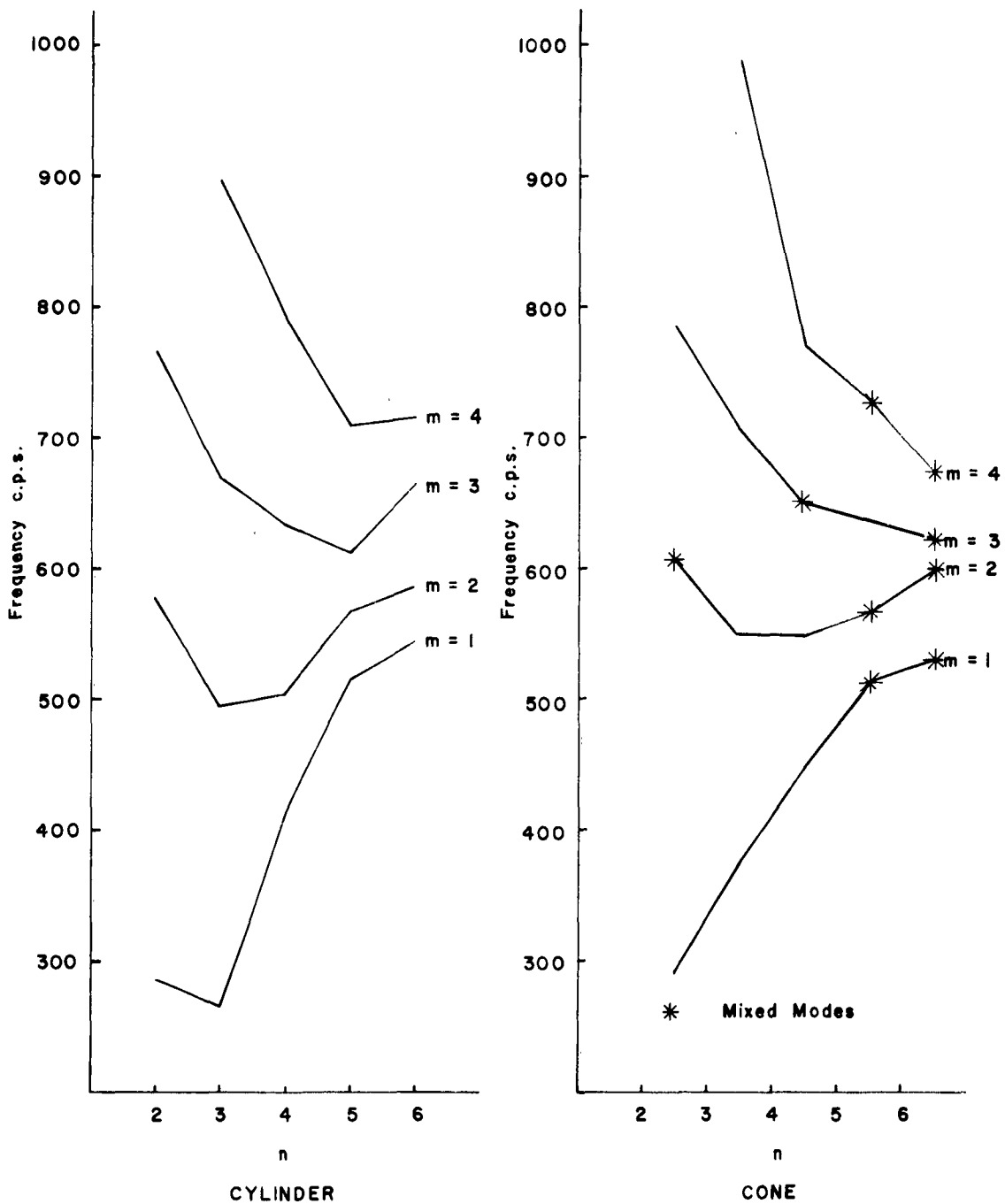


FIGURE 8 FREQUENCY VERSUS RADIAL NODES

1 / 2 " PLATE
2 " X 1 " STIFFENER

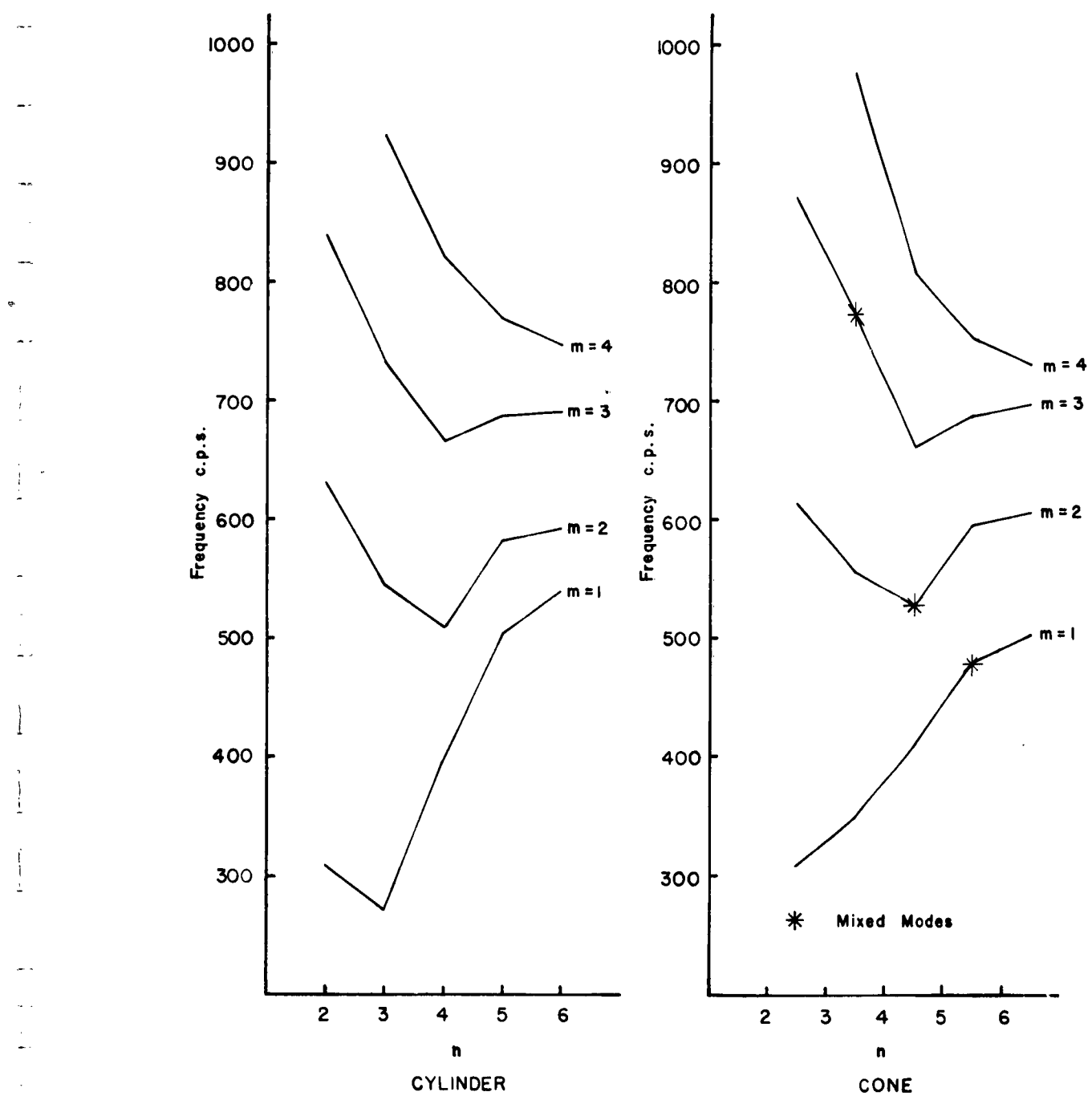
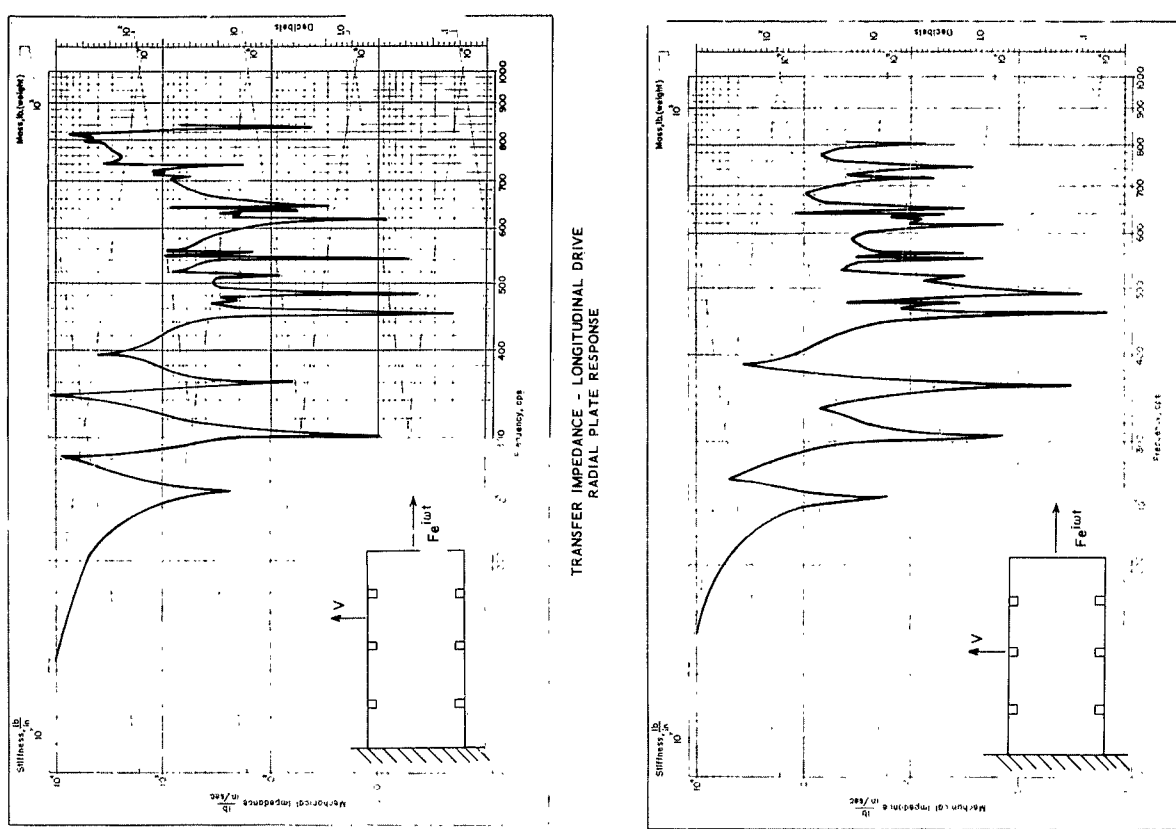
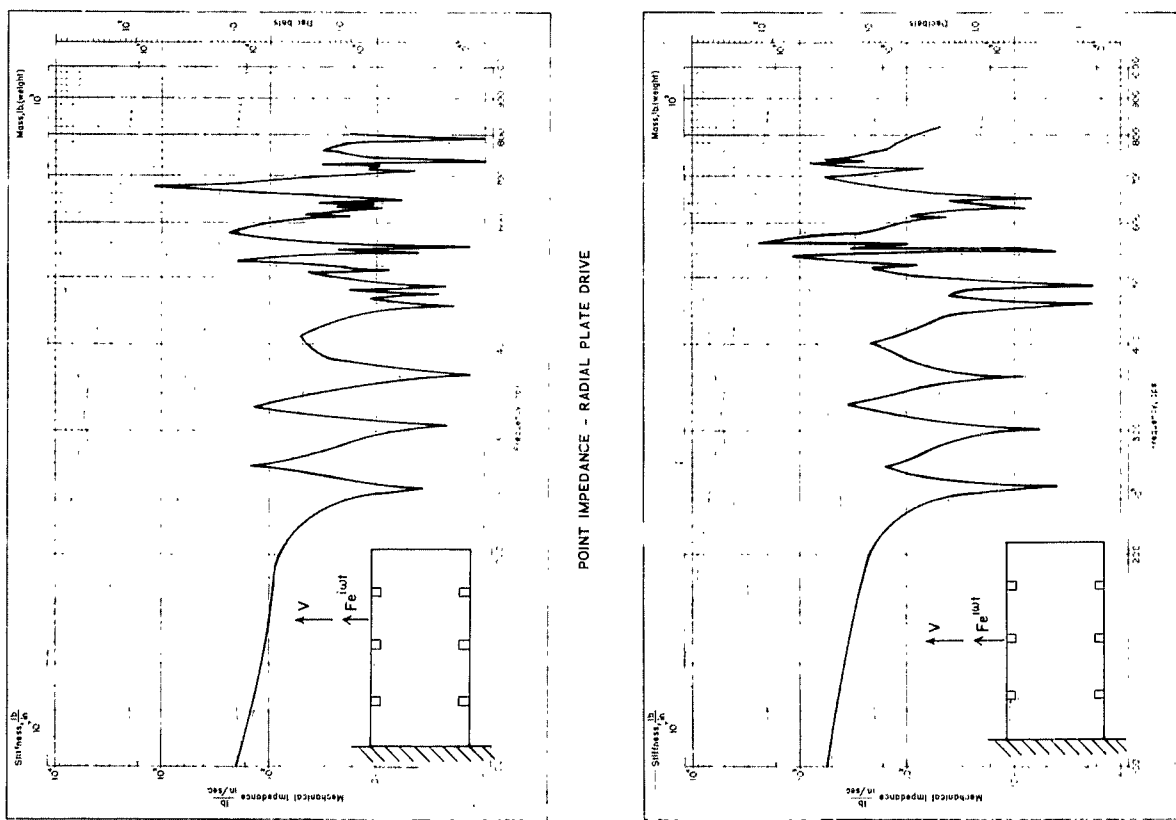


FIGURE 9 FREQUENCY VERSUS RADIAL NODES



TRANSFER IMPEDANCE - LONGITUDINAL DRIVE
RADIAL PLATE RESPONSE

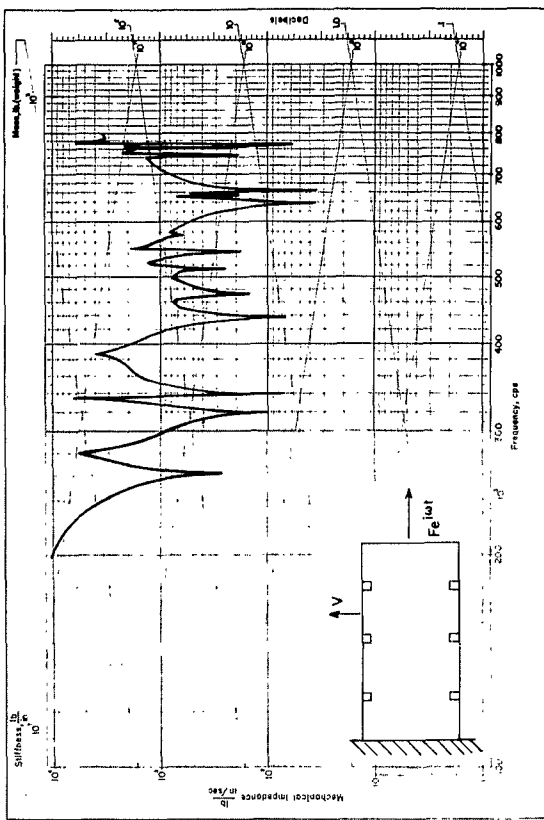


POINT IMPEDANCE - RADIAL PLATE DRIVE

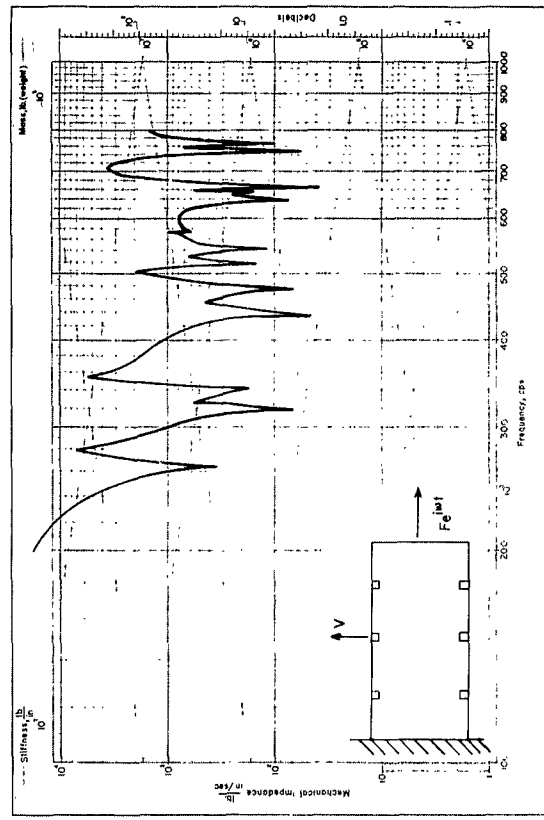
POINT IMPEDANCE - RADIAL STIFFENER DRIVE

CYLINDER
1/4" PLATE
2" X 1/2" STIFFENER

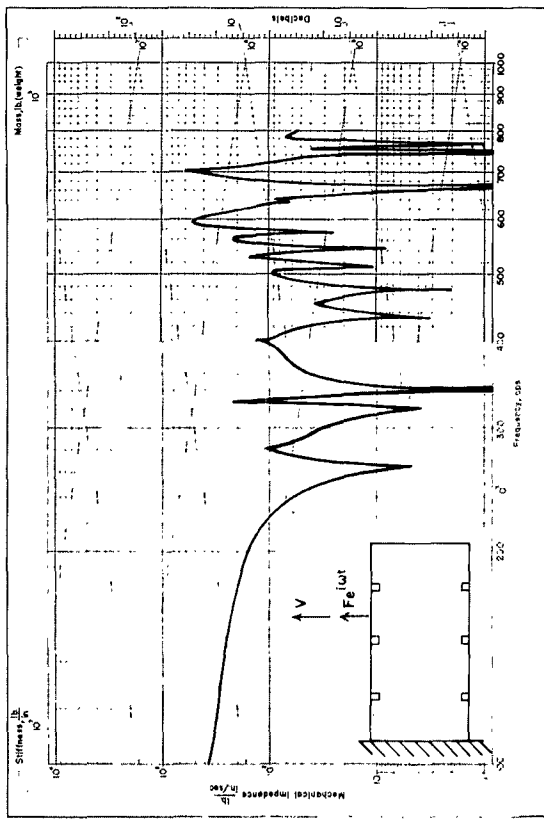
FIGURE 10



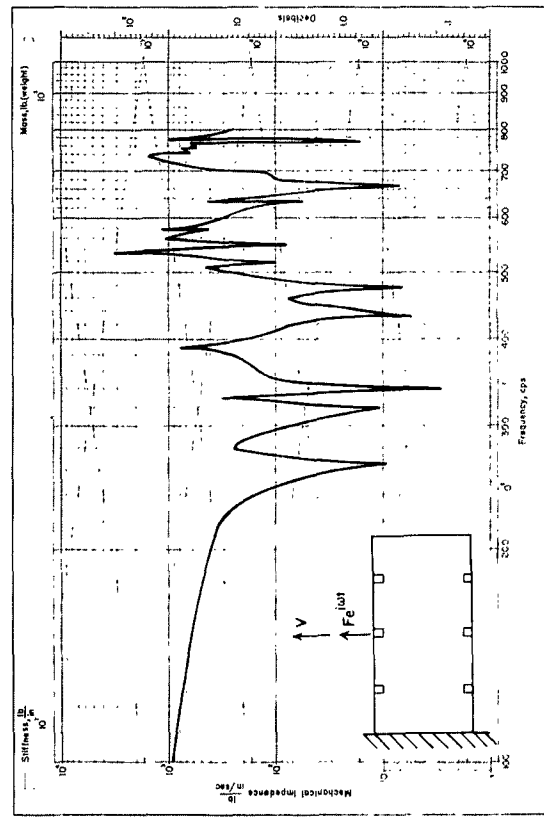
TRANSFER IMPEDANCE - LONGITUDINAL DRIVE
RADIAL PLATE RESPONSE



TRANSFER IMPEDANCE - LONGITUDINAL DRIVE
RADIAL STIFFENER RESPONSE



POINT IMPEDANCE - RADIAL PLATE DRIVE



POINT IMPEDANCE - RADIAL STIFFENER DRIVE

CYLINDER
1/2" PLATE
2" X 1/2" STIFFENER

FIGURE 11

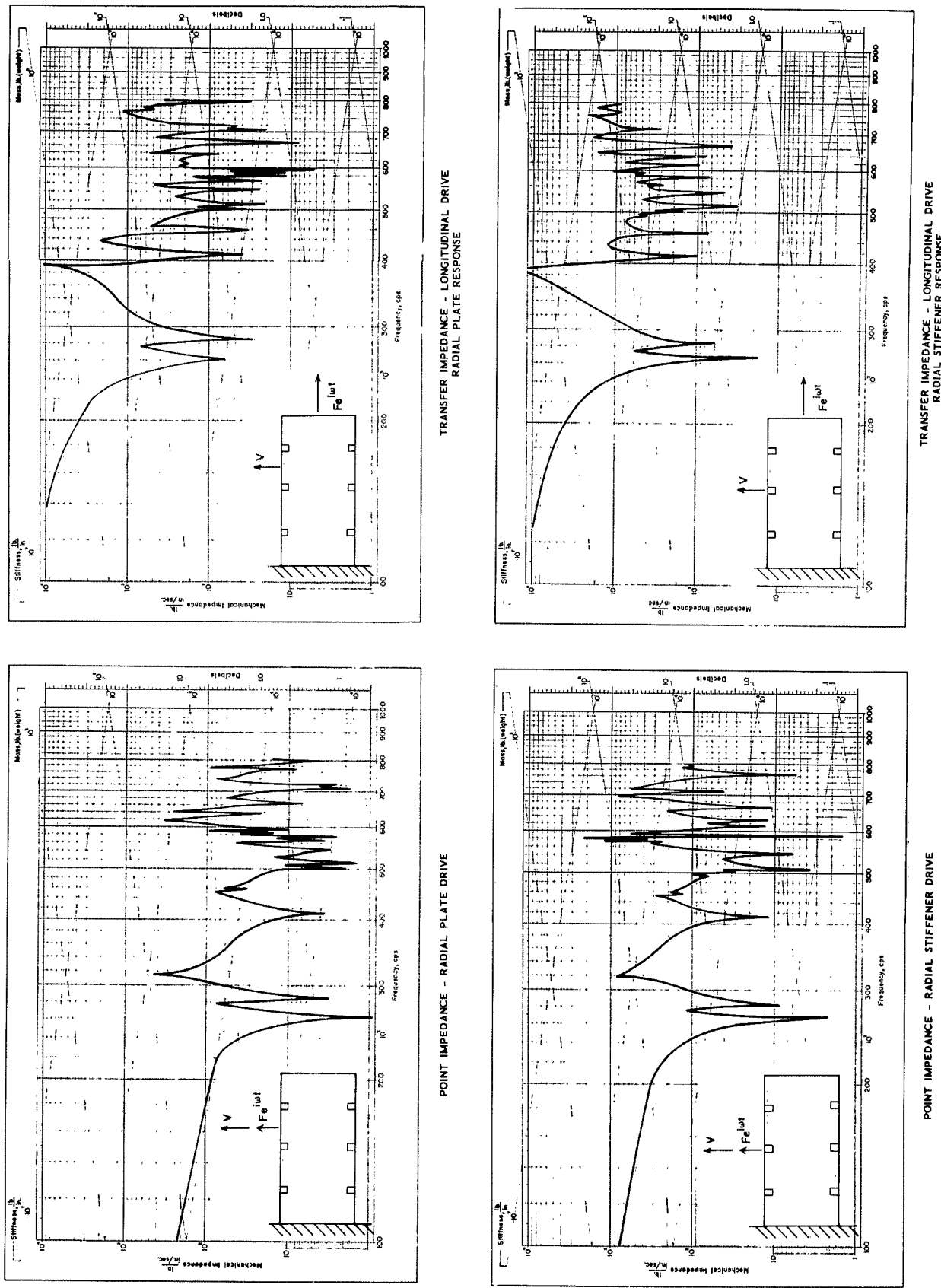
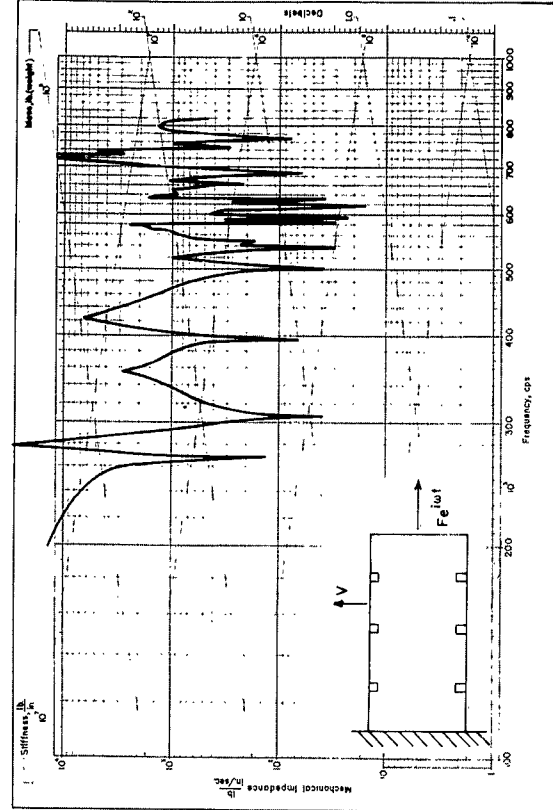
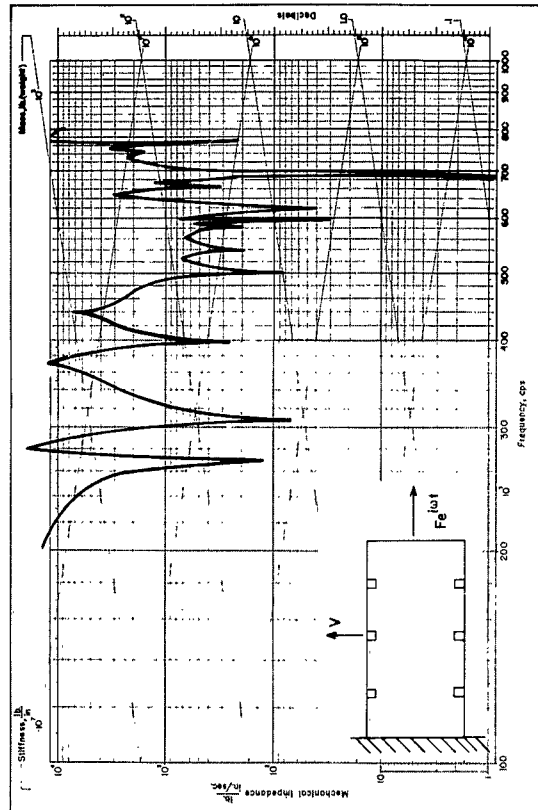


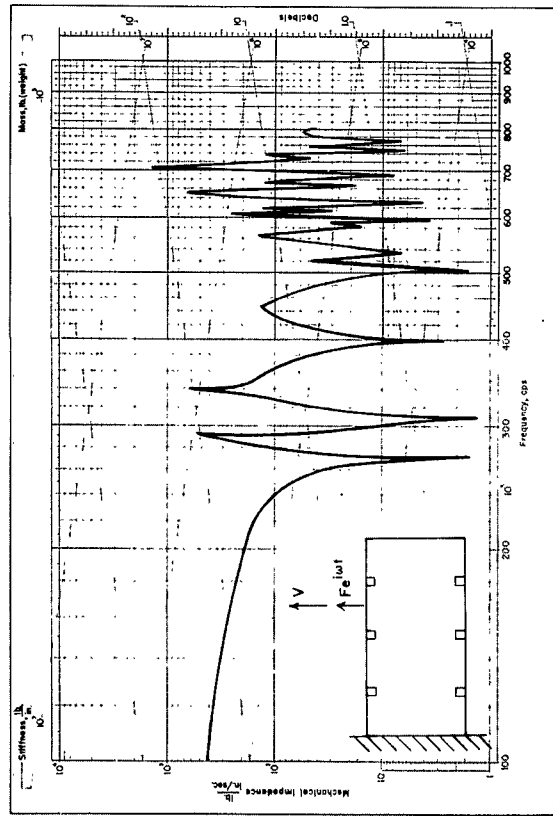
FIGURE 12



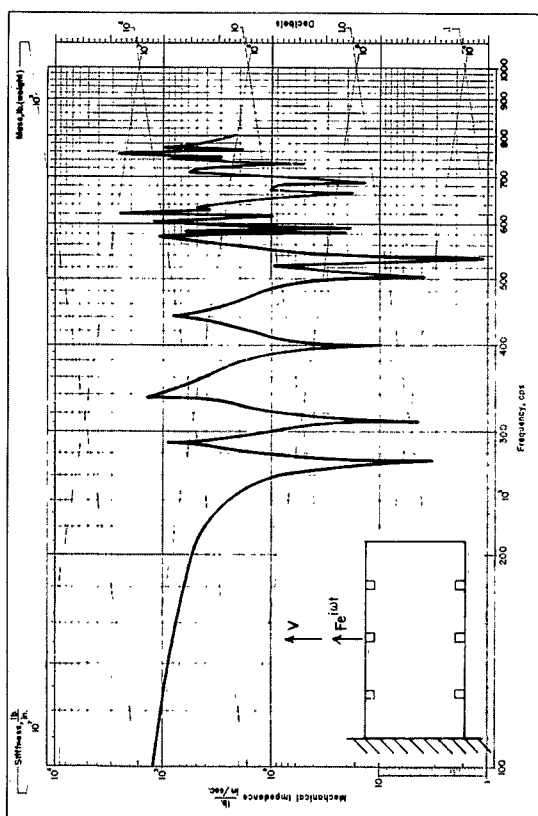
TRANSFER IMPEDANCE - LONGITUDINAL DRIVE
RADIAL PLATE RESPONSE



TRANSFER IMPEDANCE - LONGITUDINAL DRIVE
RADIAL STIFFENER RESPONSE



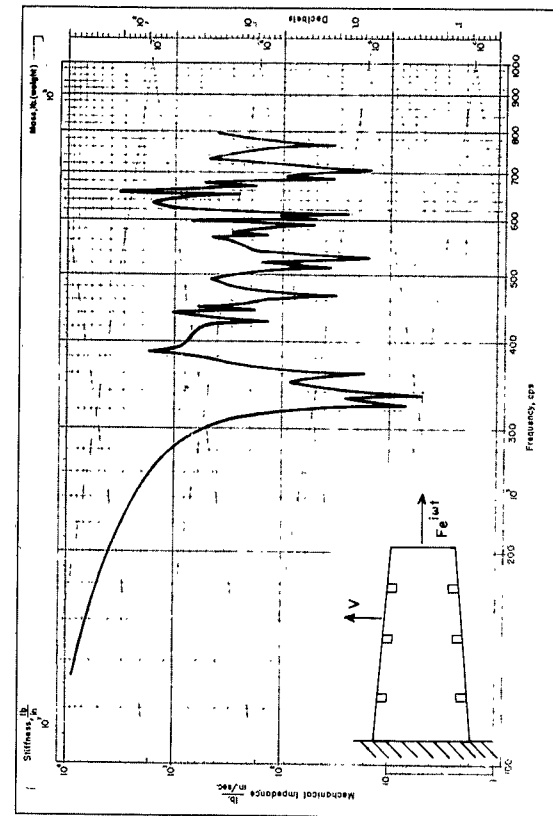
POINT IMPEDANCE - RADIAL PLATE DRIVE



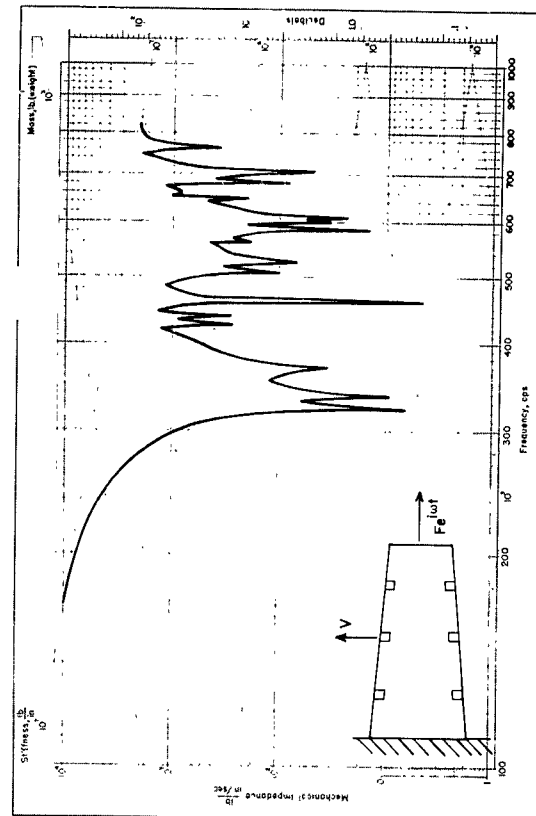
POINT IMPEDANCE - RADIAL STIFFENER DRIVE

CYLINDER
1/2" PLATE
2" X 1" STIFFENER

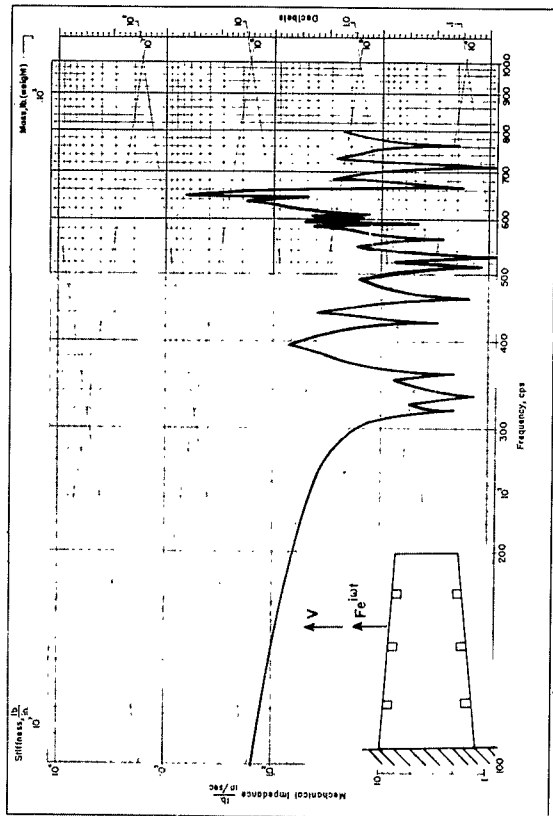
FIGURE 13



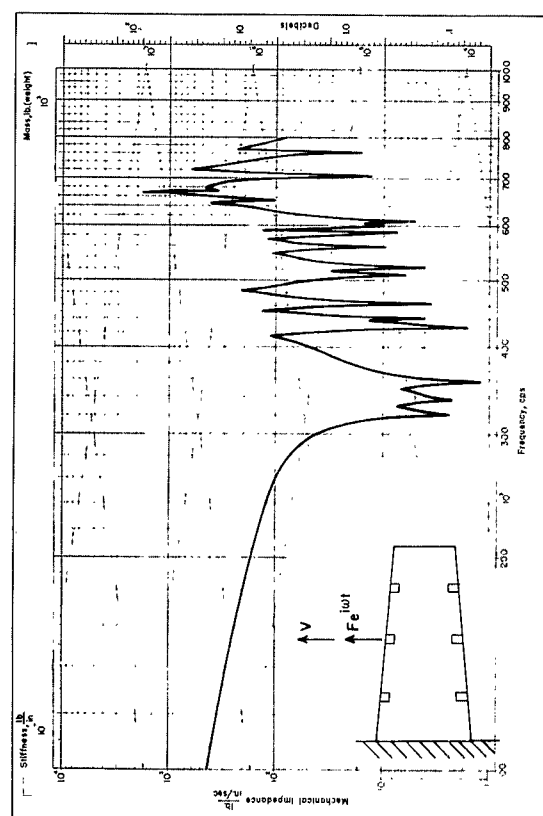
TRANSFER IMPEDANCE - LONGITUDINAL DRIVE
RADIAL PLATE RESPONSE



TRANSFER IMPEDANCE - LONGITUDINAL DRIVE
RADIAL STIFFENER RESPONSE



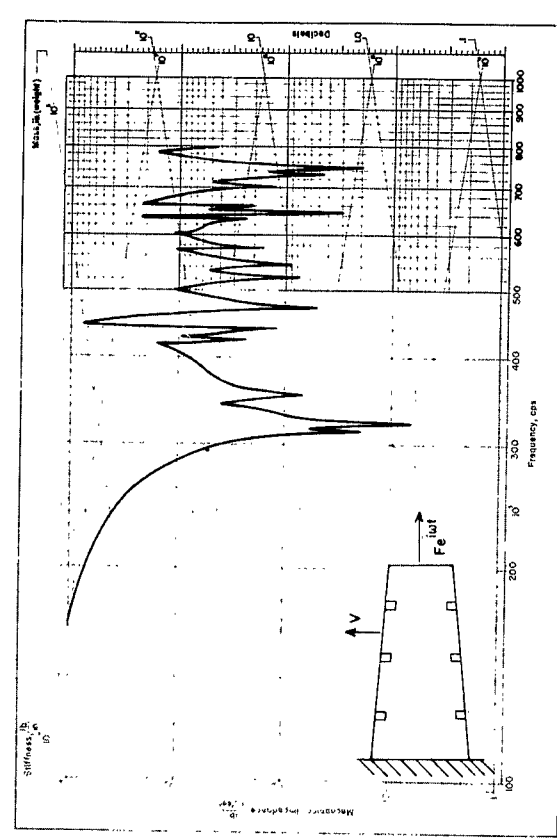
POINT IMPEDANCE - RADIAL PLATE DRIVE



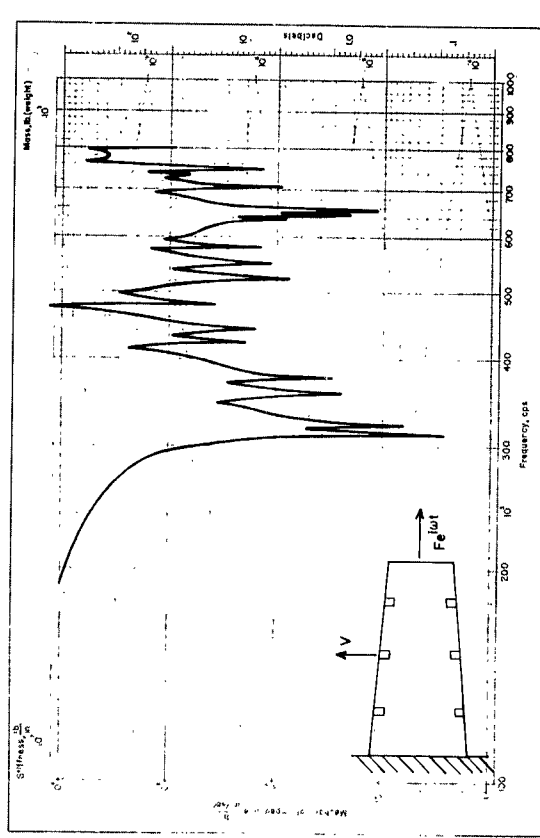
POINT IMPEDANCE - RADIAL STIFFENER DRIVE

CONE
1/4" PLATE
2" X 1/2" STIFFENER

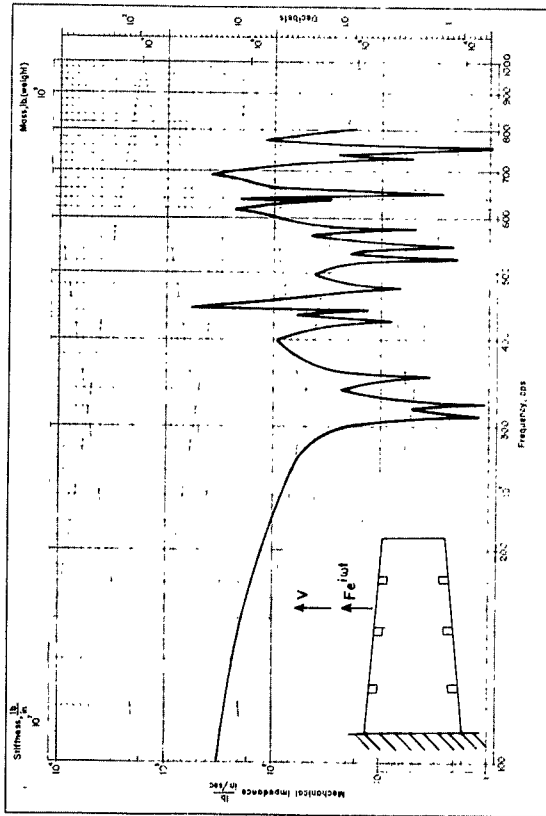
FIGURE 14



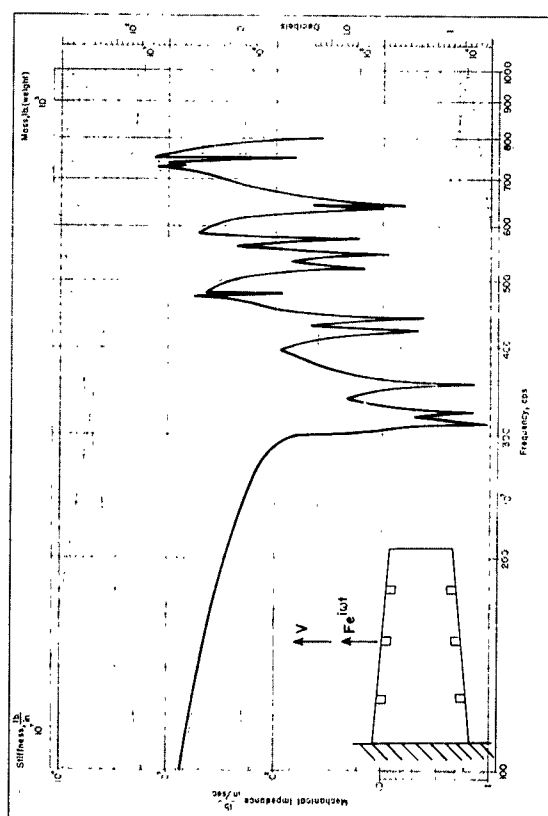
TRANSFER IMPEDANCE - LONGITUDINAL DRIVE
RADIAL PLATE RESPONSE



TRANSFER IMPEDANCE - LONGITUDINAL DRIVE
RADIAL STIFFENER RESPONSE



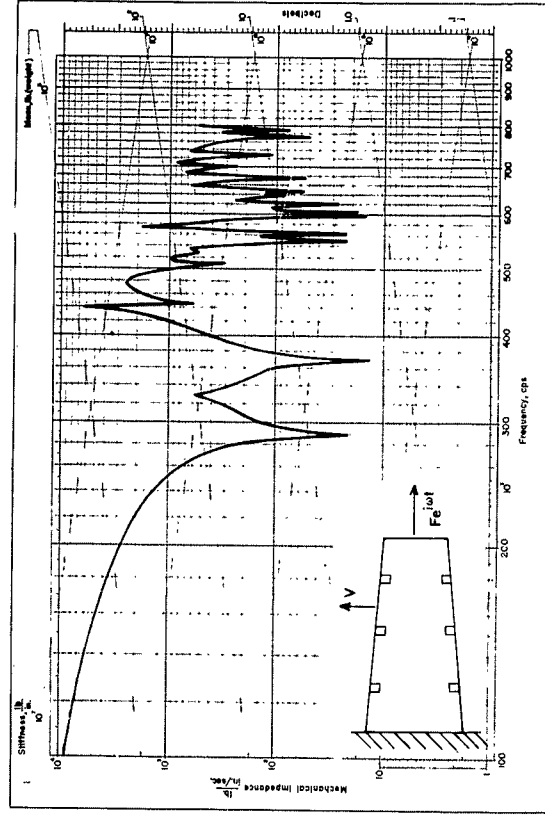
POINT IMPEDANCE - RADIAL PLATE DRIVE



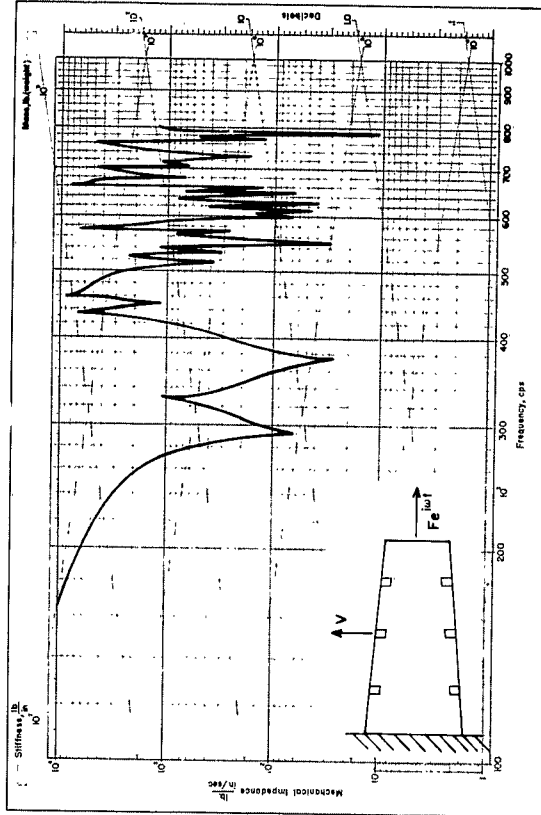
POINT IMPEDANCE - RADIAL STIFFENER DRIVE

CONE
1/2" PLATE
2" X 1/2" STIFFENER

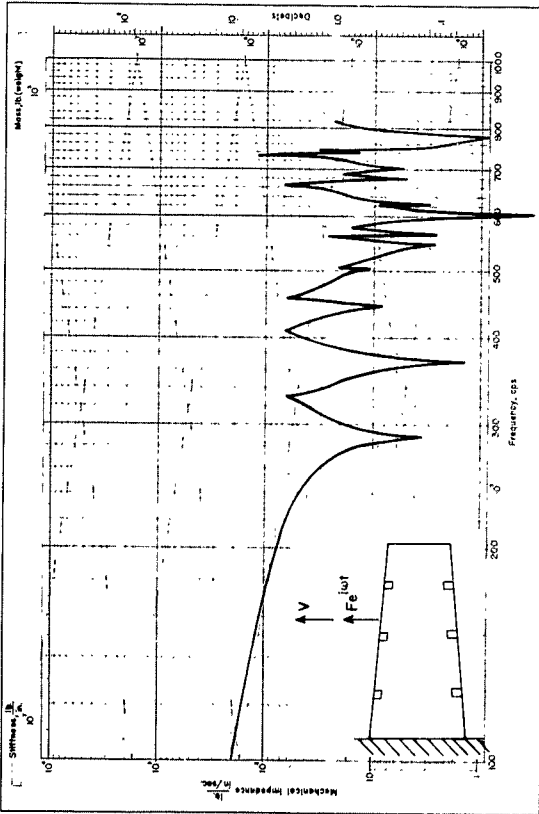
FIGURE 15



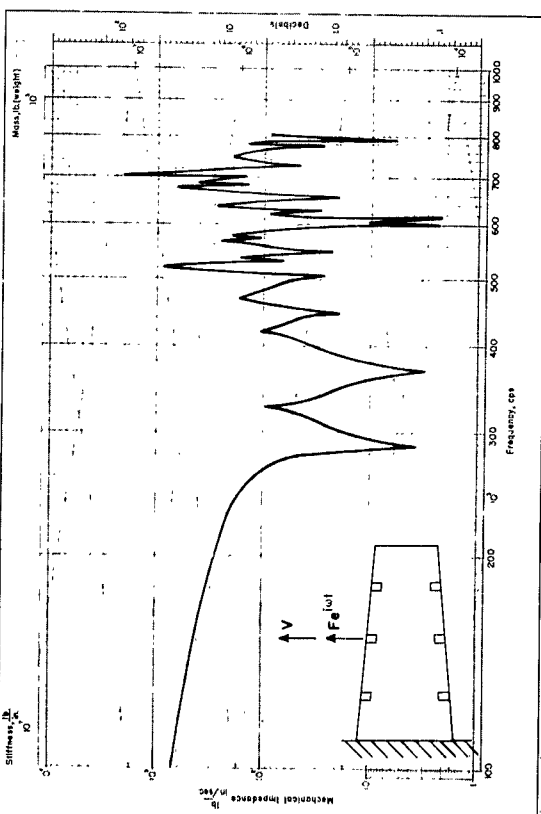
TRANSFER IMPEDANCE - LONGITUDINAL DRIVE
RADIAL PLATE RESPONSE



TRANSFER IMPEDANCE - LONGITUDINAL DRIVE
RADIAL STIFFENER RESPONSE



POINT IMPEDANCE - RADIAL PLATE DRIVE



POINT IMPEDANCE - RADIAL STIFFENER DRIVE

FIGURE 16

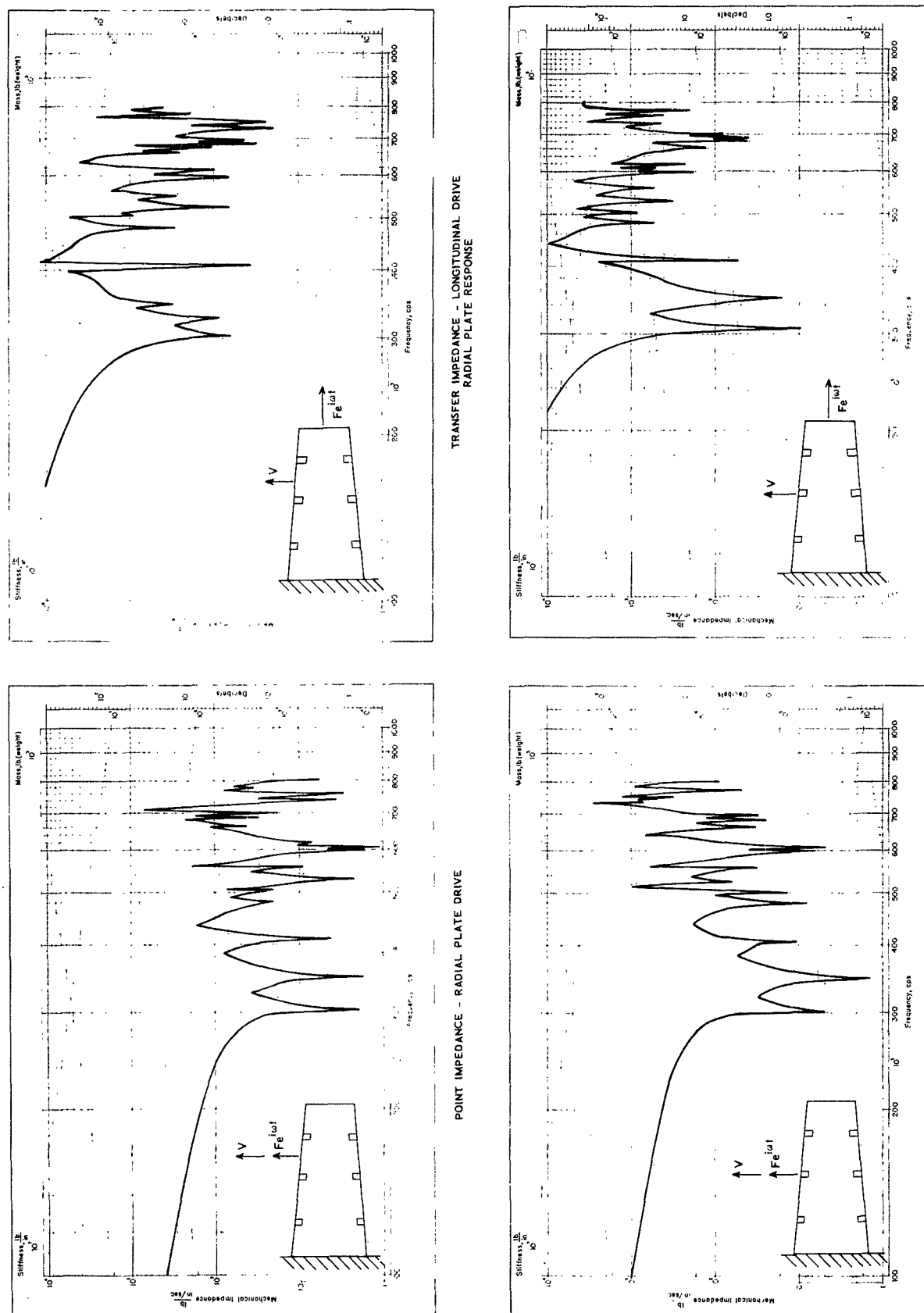


FIGURE 17

DISTRIBUTION LIST

Copies	Copies
75 Commanding Officer and Director David Taylor Model Basin Washington 7, D. C. Attn: Code 513	9 Chief, Bureau of Ships Department of the Navy Washington 25, D. C. Attn: Code 320 (Lab N.G.T.) (1) 335 (Technical Information Branch) (3)
10 Commander Armed Services Technical Information Agency Arlington Hall Station Arlington 12, Virginia Attn: TIPDR	345 (Ship Silencing Branch) (1) 420 (Preliminary De- sign Branch) (1) 421 (Preliminary De- sign Branch) (1) 440 (Hull Design Branch) (1) 442 (Scientific and Research) (1)
1 Commander Boston Naval Shipyard Boston, Massachusetts	1 Chief, Bureau of Yards and Docks Department of the Navy Washington 25, D. C. Attn: Code D-400 (Research Div.)
1 California Institute of Technology Pasadena 4, California Attn: Dr. T. Y. Wu	2 Iowa Institute of Hydraulic Research State University of Iowa Iowa City, Iowa Attn: Dr. H. Rouse, Director Dr. L. Landweber
1 Commander Charleston Naval Shipyard Charleston, South Carolina	2 Institute of Mathematical Sciences New York University 25 Waverly Place New York 3, New York Attn: Prof. J. Stoker (1) Prof. A. Peters (1)
1 Colorado State University Department of Civil Engineering Fort Collins, Colorado Attn: Mr. A. R. Chamberlain, Chief Engineering, Mathematics and Physics Research	
1 Director Davidson Laboratory Stevens Institute of Technology 711 Hudson Street Hoboken, New Jersey	

Copies		Copies
3	University of California Berkeley 5, California Attn: Department of Engineering Prof. H. A. Schade, Head Dept. of Naval Architecture (1)	1 Commander U.S. Naval Proving Ground Dahlgren, Virginia
	Prof. J. Johnson (1)	1 Commanding Officer U.S. Naval Repair Facility U.S. Naval Station San Diego, California
	Prof. J. V. Wehausen, Institute of Engineering Research (1)	1 Administrator Webb Institute of Naval Architecture Crescent Beach Road Glen Cove, Long Island, New York Attn: Technical Library
1	University of Maryland College Park, Maryland Attn: Institute for Fluid Dynamics and Applied Mathematics	1 Director Woods Hole Oceanographic Institute Woods Hole, Massachusetts Attn, Dr. C. Iselin, Senior Oceanographer
1	University of Michigan Ann Arbor, Michigan Attn: Prof. R. B. Couch, Chairman Department of Naval Architecture and Marine Engineering	1 Editor Engineering Index, Inc. 29 West 39th Street New York, New York
1	Commanding Officer Headquarters U.S. Army Transportation Command Fort Eustis, Virginia Attn: Research Reference Center	1 Librarian Society of Naval Architects and Marine Engineers 74 Trinity Place New York 6, New York
1	Maritime College State University of New York Fort Schulyer New York 65, New York Attn: Prof. J. J. Foody, Head Engineering Department	1 Commander Norfolk Naval Shipyard Portsmouth, Virginia

Copies

1 Commander
New York Naval Shipyard
Brooklyn, New York

1 New York University
University Heights
New York 53, New York
Attn: Dr. W. J. Pierson, Jr.

1 University of Notre Dame
Notre Dame, Indiana
Attn: Dr. A. G. Strandhagen
Department of Engineering
Science

1 Oceanics, Inc.
Technical Industrial Park
Plainview, Long Island, New York
Attn: Dr. P. Kaplan

1 Douglas Aircraft Company, Inc.
Aircraft Division
Long Beach, California
Attn: Mr. A. M. O. Smith

1 Technical Research Group, Inc.
2 Aerial Way
Syosset, New York
Attn: Dr. J. Kotik

1 Sibley School of Mechanical Engineering
Cornell University
Ithaca, New York
Attn: Prof. R. O. Fehr

1 Hydronautics, Incorporated
Pindell School Road
Howard County, Laurel, Maryland
Attn: Mr. P. Eisenberg

Copies

1 Pennsylvania State University
University Park, Pennsylvania
Attn: Director
Ordnance Research Laboratory

1 Commander
Philadelphia Naval Shipyard
Philadelphia, Pennsylvania

1 Illinois Institute of Technology
Technology Center
Chicago 16, Illinois
Attn: Dr. I. Michelson

1 Vidya
1450 Page Mill Road
Palo Alto, California
Attn: Dr. J. Nielsen

1 Cambridge Acoustical Associates, Inc.
129 Mount Auburn Street
Cambridge 38, Massachusetts
Attn: Dr. J. V. Rattaya

1 Bolt Beranek and Newman, Inc.
50 Moulton Street
Cambridge 38, Massachusetts
Attn: Dr. F. J. Jackson

1 Armour Research Foundation
10 West 35th Street
Chicago 16, Illinois
Attn: Mr. H. B. Karplus

1 Stanford Research Institute
Physics Division
Menlo Park, California
Attn: Dr. V. Salmon

Copies		Copies	
1	Chief of Naval Research (Code 438) Department of the Navy Washington 25, D. C.	1	Commander Long Beach Naval Shipyard Long Beach, California
2	Chief, Bureau of Naval Weapons (R) Department of the Navy Washington 25, D. C.	1	Commander Mare Island Naval Shipyard Vallejo, California
1	Special Projects Office Department of the Navy Washington 25, D. C. Attn: Chief Scientist	1	Administrator U.S. Maritime Administrator Department of Commerce Washington 25, D. C. Attn: Mr. Vito L. Russo, Deputy Chief, Office of Ship Construction
1	Commander Portsmouth Naval Shipyard Portsmouth, New Hampshire	2	U.S. Coast Guard 1300 E Street, N.W. Washington 25, D. C. Attn: Secretary, Ship Structure Committee (1) Commandant (1)
1	Commander Puget Sound Naval Shipyard Bremerton, Washington	1	Chief, Applied Naval Architecture Department of Nautical Science U.S. Merchant Marine Academy Kings Point, Long Island, New York
1	Commander San Francisco Naval Shipyard San Francisco, California	1	Superintendent U.S. Naval Academy Annapolis, Maryland Attn: Library
1	Society of Naval Architects and Marine Engineers 74 Trinity Place New York 6, New York	1	Superintendent U.S. Naval Postgraduate School Monterey, California
1	Dr. L. C. Straub, Director St. Anthony Falls Hydraulic Laboratory University of Minnesota Minneapolis 14, Minnesota		

Copies

- 1 Massachusetts Institute of
Technology
Cambridge 39, Massachusetts
Attn: Department of Naval
Architecture and
Marine Engineering
- 1 Commander
Military Sea Transportation Service
Department of the Navy
3800 Newark Street, N.W.
Washington 25, D. C.
- 1 Director
National Aeronautics and Space
Administration
1512 H Street, N.W.
Washington 25, D. C.
- 1 Director
National Bureau of Standards
Washington 25, D. C.
Attn: Dr. G. B. Schubauer
(Fluid Mechanics)
- 1 Director
National Science Foundation
1951 Constitution Avenue, N.W.
Washington, D. C.
- 6 Director
U.S. Naval Research Laboratory
Code 2020
Washington 25, D. C.

Copies

- 25 Commanding Officer
Office of Naval Research
Navy 100, Fleet Post Office
New York, New York
- 1 Commanding Officer
Office of Naval Research Branch
Office
1000 Geary Street
San Francisco 9, California
- 1 Commanding Officer
Office of Naval Research Branch
Office
1030 East Green Street
Pasadena 1, California
- 1 Commanding Officer
Office of Naval Research Branch
Office
346 Broadway
New York 13, New York
- 1 Commanding Officer
Office of Naval Research Branch
Office
The John Crerar Library Building
85 East Randolph Street
Chicago 1, Illinois
- 1 Commander
Pearl Harbor Naval Shipyard
Navy 120, Fleet Post Office
San Francisco, California